

DESIGN CONSIDERATIONS FOR INTERMITTENTLY CONNECTED  
ENERGY HARVESTING WIRELESS SENSOR NETWORKS

by

Md Majharul Islam Rajib

A dissertation submitted to the faculty of  
The University of North Carolina at Charlotte  
in partial fulfillment of the requirements  
for the degree of Doctor of Philosophy in  
Electrical Engineering

Charlotte

2018

Approved by:

---

Dr. Asis Nasipuri

---

Dr. Jiang Xie

---

Dr. Yu Wang

---

Dr. Srinivas S. Pulugurtha

©2018  
Md Majharul Islam Rajib  
ALL RIGHTS RESERVED

## ABSTRACT

MD MAJHARUL ISLAM RAJIB. Design Considerations for Intermittently Connected Energy Harvesting Wireless Sensor Networks. (Under the direction of DR. ASIS NASIPURI)

Wireless sensor networks can potentially achieve perpetual maintenance-free operation by harnessing ambient energy from the environment. However, most environmental energy sources, such as vibrations, heat, radio frequency (RF) are usually inadequate and sporadic in nature. Therefore, sensor nodes that rely solely on such environmental resources, suffer from frequent and random energy outages. This energy outage leads to intermittent connectivity and induces a large delay in multi-hop transmission paradigms.

The objective of this research is to minimize the end-to-end latency due to this intermittent connectivity. In order to address this problem, several approaches are explored. First, cooperative relaying is investigated as a potential mechanism for reducing the transmission delay. The latency associated with cooperative relaying over unicast routes is analyzed and a novel scheme is proposed to improve the performance of cooperative relaying in a more practical multi-hop setting. Next, a predictive retransmission strategy is developed to find the best retransmission intervals that maximize the success probability associated with each transmission. This strategy is then adapted to two different asynchronous routing protocols: cooperative relaying over unicast routes and opportunistic routing. Finally, the delay characteristics of RF energy harvesting sensor networks is explored and analytical models are formulated to reduce delay by efficiently distributing packet forwarding load between the transmitter and receiver nodes. Performance evaluations from the theoretical models and simulations show that the proposed methods can significantly improve the delay performance in comparison to existing solutions.

## ACKNOWLEDGEMENTS

I would like to start by expressing my sincere gratitude to my advisor Prof. Asis Nasipuri, for his immense support and guidance throughout my Ph.D. years. He has helped me to identify key research issues, patiently spent countless hours to discuss and refine my cluttered ideas, and equipped me with the necessary tools to become an independent researcher.

Thanks to my dissertation committee members, Prof. Jiang (Linda) Xie, Prof. Yu Wang, and Prof. Srinivas Pulugurtha for their suggestions and encouragement, and their willingness to squeeze their schedules to accommodate my requests.

I would like to thank my friends: Ji Li, Md Shakawat Hossan, Morium Bably, Yiqian Li, Sayali Nimkar and many other graduate students for all their help. Their company has made my Ph.D. life both fun and rewarding. Thanks also to my family members who have supported me with their encouragement and best wishes.

Finally, special thanks to my wife Wahida Nasrin for her love and patience. For all the time I needed a close friend, a family member, a colleague, or a brain, she was there. I couldn't have done this without her.



## TABLE OF CONTENTS

LIST OF FIGURES	vii
LIST OF TABLES	x
CHAPTER 1: INTRODUCTION	1
1.1. Intermittent Connectivity in Energy Harvesting Paradigm	1
1.2. Research Outline	3
1.3. Organization of the Dissertation	8
CHAPTER 2: RELATED WORK	9
2.1. Energy Harvesting in Wireless Sensor Networks	9
2.1.1. RF Energy Harvesting	11
2.2. Delay Minimization in Energy Harvesting ICSN	14
2.2.1. MAC Layer Design	14
2.2.2. Routing Layer Design	20
CHAPTER 3: MINIMIZING DELAY USING TIME DIVERSITY	24
3.1. Analysis of Delay with Cooperative Relaying	25
3.1.1. Preliminaries	26
3.1.2. Analytical Model	27
3.2. Ephemeral Two-hop Opportunistic Cooperation (ETOC)	34
3.3. Performance Results	36
CHAPTER 4: ACHIEVING LOW LATENCY THROUGH TRANSMISSION TIME ESTIMATION	39
4.1. Predictive Retransmission for Intermittent Wireless Links	39
4.1.1. Energy Dynamics of a Sensor Node	40

4.1.2.	Optimal Retransmission Interval	43
4.1.3.	Delay Analysis	49
4.2.	Cross-layer design with predictive retransmission and transmission Diversity	53
4.2.1.	Cooperative Relaying with Predictive Retransmissions	53
4.2.2.	Opportunistic Routing with Predictive Retransmissions	55
4.3.	Simulation Results	55
4.3.1.	Event Monitoring: Single Packet Stream	56
4.3.2.	Event Monitoring: Overlapping Packet Stream	58
4.3.3.	Event Monitoring: Random Node Topology	60
4.3.4.	Data Collection	61
CHAPTER 5: DELAY MINIMIZATION IN RF ENERGY HARVESTING SENSOR NETWORKS		63
5.1.	Delay Characteristics and Motivation	64
5.2.	Parent vs Child Triggered Data Transmission	66
5.2.1.	Success Probability of Parent vs Child Triggered Transmission	69
5.3.	Optimal Energy Allocation Between the Transmission and Reception Activities	76
5.3.1.	Optimal Policy	77
5.3.2.	Data Rate of the Child-parent and the Parent-sink Links	78
CHAPTER 6: CONCLUSIONS		82
REFERENCES		85

## LIST OF FIGURES

FIGURE 1.1: A typical sensor network deployed for event monitoring.	2
FIGURE 1.2: Packet forwarding delay in an intermittently connected link.	3
FIGURE 1.3: Research outline.	7
FIGURE 2.1: Operation of (a) B-MAC (b) X-MAC.	15
FIGURE 2.2: Operation of (a) opportunistic routing and (b) unicast routing with cooperative relaying in an intermittently connected network.	22
FIGURE 3.1: (a) System states of a node (b) how transmitter and receiver communicate while going through different states.	25
FIGURE 3.2: Illustration of the reduction of transmission delay in ICSNs using neighbor cooperation.	26
FIGURE 3.3: States of the Markov Chain.	29
FIGURE 3.4: Comparison between theoretical model and simulation.	33
FIGURE 3.5: (a)Wasting next-hop parents energy, (b)deteriorating energy of two-hop parent, (c)energy wastage surrounding the sink node.	34
FIGURE 3.6: Network model used for simulation experiments.	37
FIGURE 3.7: Delay improvement from cooperation.	37
FIGURE 4.1: Illustration of (a) back-to-back and (b) predictive retransmissions.	40
FIGURE 4.2: Continuous time representation (top) and its discrete time approximation (bottom) of the variation of energy level in a rechargeable sensor node.	41
FIGURE 4.3: Finding the optimal retransmission interval.	43
FIGURE 4.4: Probability of success of packet retransmissions in an intermittently connected wireless link using different retransmission intervals.	46

FIGURE 4.5: Maximum success probability achievable using predictive and back-to-back retransmissions in an intermittently connected wireless link.	47
FIGURE 4.6: Calculation of the packet transmission delay.	50
FIGURE 4.7: Delay performance in an intermittently connected wireless link using predictive and back-to-back retransmissions.	52
FIGURE 4.8: Delay performance in intermittently connected wireless link using cooperative relaying with different retransmission policies.	54
FIGURE 4.9: Delay performance for single packet stream in event monitoring application.	58
FIGURE 4.10: Delay performance for multiple stream in event monitoring application.	59
FIGURE 4.11: Delay performance for event monitoring application with random topology. Here, a) node configuration for the simulation, and b) end-to-end delay performance.	60
FIGURE 4.12: Delay performance for data collection application. Here, a) node configuration for the simulation, b) delay at various harvested energy amounts, and c) packet loss rate with finite buffer size.	62
FIGURE 5.1: Received power and harvesting characteristics at different distances from the RF source.	65
FIGURE 5.2: Node configuration for RF energy harvesting simulation.	67
FIGURE 5.3: a) Traffic load b) received power c) end-to-end latency and d) average retransmissions per packet at different hop distances from the sink.	68
FIGURE 5.4: a) Parent triggered data transmission b) child triggered data transmission.	69
FIGURE 5.5: Energy consumption at various section of the active period.	70
FIGURE 5.6: Scenario where nodes randomly wake up within a slot.	72
FIGURE 5.7: For child vs parent initiated transmissions a) variations in meeting effort durations b) mean time to overlap.	72

FIGURE 5.8: Success probability estimation.	73
FIGURE 5.9: Maximizing the likelihood of a successful transmission.	74
FIGURE 5.10: Probability of success with a) variable time elapsed since last schedule exchange b) different parent distances from sink.	76
FIGURE 5.11: Optimizing throughput by effectively distributing parents energy.	77
FIGURE 5.12: Bit rate of the child-parent and parent-sink link for different fractions of the parent's energy spend in transmission.	80
FIGURE 5.13: Maximum achievable throughput and the fraction of energy should be spent to sustain that.	81

## LIST OF TABLES

TABLE 3.1: Parameters used in the analysis for cooperative relaying.	33
TABLE 4.1: Notations used in formulating optimal retransmission intervals.	42
TABLE 4.2: Node parameters used for demonstrating the optimum retransmission interval characteristics.	47
TABLE 4.3: Simulation parameters used for evaluating the performance of the predictive retransmission scheme.	57
TABLE 5.1: Simulation parameters used for demonstrating RF energy harvesting ICSN characteristics.	66

## CHAPTER 1: INTRODUCTION

A wireless sensor network (WSN) is a network of many low power, distributed embedded devices that can sense their environment and wirelessly transfer the information to a remote data sink through multi-hop routing. These devices are equipped with low power microcontrollers that can perform basic data processing and implement lightweight wireless protocol stacks. They also have various environmental sensors and a transceiver module for wireless communication. An onboard energy supply such as a primary (non-rechargeable) battery or supercapacitor powers the whole device. Once deployed, these devices autonomously form an ad-hoc network, usually through a tree topology rooted at the sink as illustrated in Fig. 1.1. WSNs offer a low cost, adaptive, and distributed monitoring solution that can be conveniently deployed over wide geographical regions and hard to access places. However, the logistical cost of periodically replacing batteries is the main deterrent for using them for long-term monitoring applications.

### 1.1 Intermittent Connectivity in Energy Harvesting Paradigm

Finite, single-use onboard energy resources such as batteries in Wireless Sensor Nodes continue to be the key challenge in achieving long-term maintenance-free operation. To address this challenge, earlier research efforts were focused on energy conservation techniques [1, 2] using single-use batteries. This includes optimizing the lowest layer through transmission power control or modulation optimization etc, routing and MAC layer through duty cycling, energy efficient routing strategies, and application layer data aggregation, storage, and adaptive sampling just to name a few. However, long-term sustainability of Wireless Sensor Networks can only be achieved

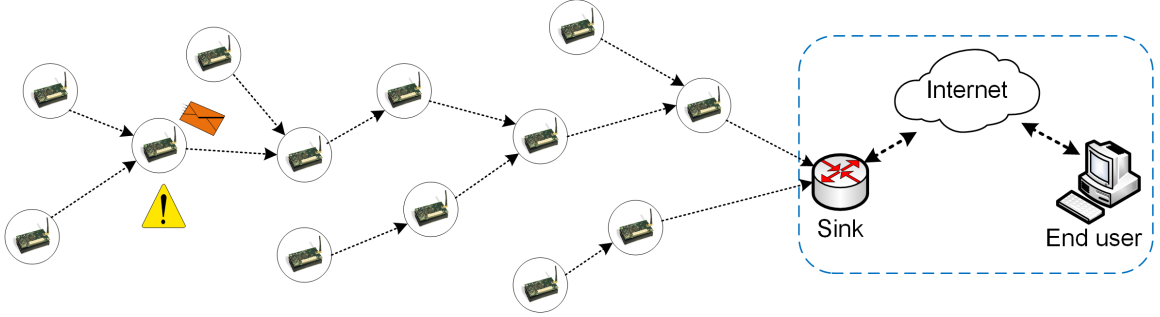


Figure 1.1: A typical sensor network deployed for event monitoring.

if the sensor nodes do not have to rely on batteries. This has triggered wide interest in ambient energy-harvesting technologies for wireless sensor nodes [3–6]. The goal is to achieve a batteryless operation, where nodes harvest energy from the environment and use short-term reliable storages such as super-capacitors or solid state batteries. However, a key problem is that environmental energy sources such as light, mechanical vibrations, radio frequency (RF), heat etc. are highly unpredictable and sporadic in nature [7–9]. In addition, the amount of energy available from these sources is usually limited. In some cases, the available power from environmental harvesting devices may be significantly lower than that required for continuous operations. Examples include vibration energy harvesting and RF energy. The random availability of energy sources coupled with limitations of supply and storage makes it difficult to operate the wireless sensor nodes continuously for extended periods of time. Consequently, sensor nodes in such batteryless WSNs may frequently have to shut down their power-hungry components such as the radio and go into a deep-sleep mode until they recharge up to a certain level to become active again. This gives rise to intermittent connectivity in WSNs, where the wireless nodes experience random and asynchronous outages [10].

Message delivery in such *intermittently connected sensor networks (ICSN)* pose several challenges. First, the asynchronous nature of the sleep-wake periods of the nodes makes it difficult to implement fixed scheduling schemes, which is one of the



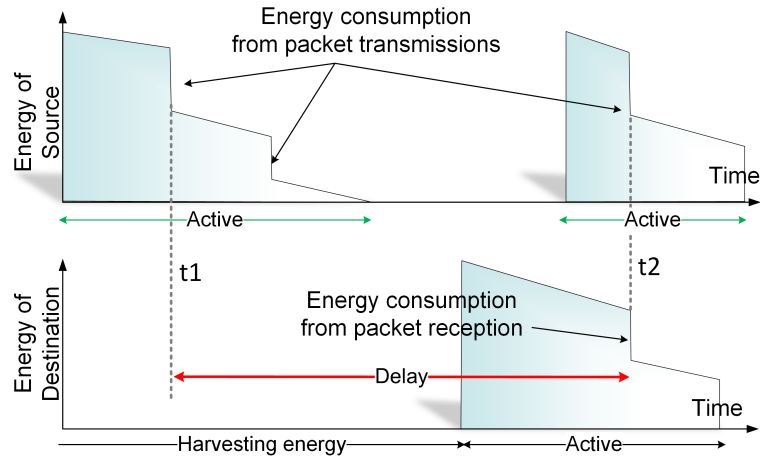


Figure 1.2: Packet forwarding delay in an intermittently connected link.

mechanisms that can be applied for achieving reliable data transfer with limited energy wastage. Second, unlike in non-rechargeable sensor networks where reliability is achieved primarily by extending the battery life using energy conservation methods, here more aggressive communication strategies are required that are closely tied to the characteristics of energy harvesting and consumption in the sensor nodes. This is because of the fact that energy storage devices such as super-capacitors and solid-state batteries have limited storage and high leakage, leading to energy wastage without use. Third, in some scenarios such as RF energy harvesting networks, the amount of harvestable energy is highly correlated to the spatio-temporal property of the node making message forwarding capabilities non-uniform. Consequently, the achievement of low latency communications in ICSNs requires efficient utilization of the active periods of the nodes that depend on the energy arrival and consumption characteristics.

## 1.2 Research Outline

To better understand the packet forwarding delay in an intermittently connected network, let's consider a link consisting of a single source-destination pair. The energy dynamics of this pair is illustrated in Fig. 1.2. Initially, the source has sufficient energy to perform packet transmission whereas the destination does not have enough

energy for the reception and it is in the inactive harvest mode. The source repeatedly attempts to forward a packet but all of its transmission attempts are wasted due to the dormancy of the receiver. Because of the high energy cost of transmissions, the source quickly depletes all of its energy and goes into inactive mode. After a while (usually, this period is long since the energy replenish rate is low), both the source and destination accumulate a certain level of energy and resume their normal operation. This time when the source transmits, the destination can receive the packet, and the packet forwarding is completed. Since the probability that both the source and the destination's active periods overlap is very low in an intermittently connected network, the delay involved in forwarding a packet is significantly large.

In this research, we concentrate on the design considerations for reducing delay in ICSNs. Specifically, we develop strategies for MAC and routing layers to benefit from the energy harvesting characteristics and reduce the end-to-end latency over multi-hop routes. Two types of ICSNs are considered. In the first type, nodes experience independent and identically distributed random energy outages due to randomness (mostly uncorrelated) in their energy arrival. Examples of such ICSNs are where nodes harvest energy from vibrations caused by passing vehicles [9] or piezoelectric stress generated from human footsteps [11]. The second type of ICSNs where the energy outages in the nodes are relatively predictable but have a very high spatial correlation. RF energy harvesting networks which are attracting increasing attention, fall in this category [12]. Our design approaches to minimize delay in these ICSNs are discussed below,

- **Delay minimization through transmit time diversity:** In ICSN, each node goes through random periods of active and deep-sleep cycles. When a node blindly tries to forward a packet i.e., without any knowledge of the active state of the receiver, it can enhance the success probability by increasing and spreading out the total number of delivery attempts. Since energy harvesting

is limited, the number of attempts can only be increased with the help of other nodes by either increasing the number of sources independently trying to forward the same packet or by increasing the number of independent potential receivers willing to receive the same packets. The randomness of active periods in these additional nodes will automatically spread out the attempts. We leverage these concepts to minimize the link delay with cooperative relaying over unicast routes and opportunistic routing. In cooperative relaying, when a node's transmission attempt fails to reach the desired destination, and a common neighbor (neighbor to both source and destination nodes) node overhears the packet, it offers to cooperate by independently forwarding the packet on behalf of the source node. Cooperative relaying improves energy utilization by tapping into the energy resources of idle nodes in the vicinity of the source and destination, some of this energy would otherwise be wasted due to ambient processes, such as overhearing or leakage. Opportunistic routing is the process by which any node that receives a packet attempts to forward it to another node that is closer to the destination. As discussed in the next chapter, opportunistic routing has received considerably more attention in the literature compared to unicast routing with cooperative relaying. Hence, we first develop a stochastic model to quantify the performance improvement achievable from cooperative relaying. Then, we propose a cooperative relaying based two-hop routing protocol that further minimizes the delay in a multi-hop network.

- **Delay minimization through predictive retransmission interval:** The harvest rates in ICSNs are usually minuscule, and therefore, the deep-sleep phases (for harvesting energy) are long and can significantly affect the overall delay performance. After each deep-sleep phase, the source nodes wake up to make a handful transmissions attempts with the limited amount of energy they harvested. If the success probabilities from these attempts are low, they again

have to go through the long deep-sleep mode and wait for the next set of attempts. In this research, we increase the success probability of each attempt by optimizing the retransmission interval, and consequently, reduce the number of long futile waiting periods. The idea is to *predict the best time for a retransmission* after each failed transmission that maximizes the probability of successfully reaching a destination. We recognize this as an important parameter since the optimum retransmission interval can potentially minimize energy wastage caused by unsuccessful retransmissions that increases with excessively small retransmission intervals at the same time reducing the probability of missing the active window of the receiver, which eventually leads to a longer average delay. We present a probabilistic model to find this optimal packet retransmission times. Our prediction strategy is based on the energy arrival rate as well as node's activities such as transmission, reception, and sensing to reflect the real-life scenario. We also develop a mathematical formulation to estimate the expected delay and use simulations to evaluate the delay characteristics of the proposed model. Finally, we integrate this predictive schemes in both unicast routing with cooperative relaying and opportunistic routing protocols to minimize the end-to-end latency.

- **Delay minimization by parent assisted data transmission process:** IC-SNs where RF energy harvesting is the principal mean for energy supply, exhibits a unique property- node's energy harvest rate is highly dependent on the proximity to the RF energy source [13, 14]. Often this RF energy source is located at the sink which makes the parent nodes significantly more capable of handling traffic (transmission and reception) compared to their children. This is rather desirable since parents not only have to forward its own traffic but also children's traffic as well. Interestingly, our study shows that the amount of energy children have to spend for forwarding packet is much higher than its par-

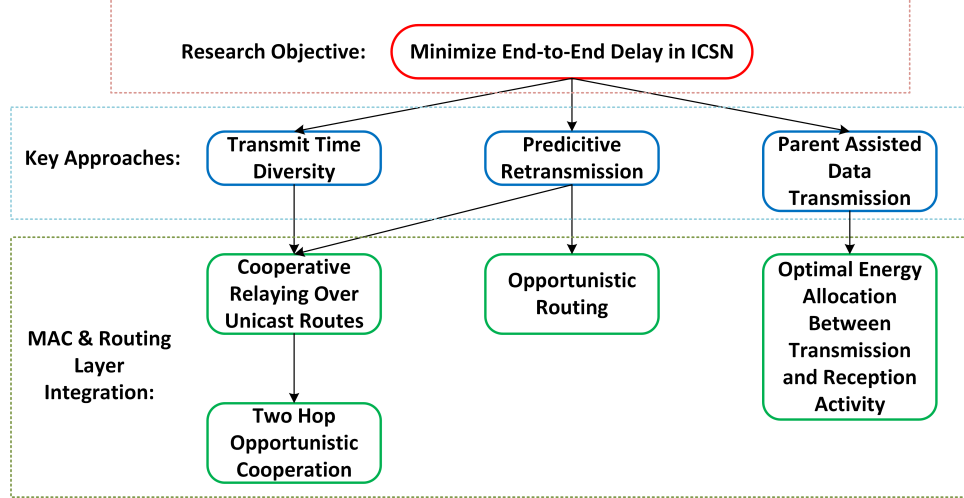


Figure 1.3: Research outline.

ent. This high energy cost combined with lower harvest rate makes children's traffic more susceptible to a longer delay. This becomes severe as the child's distance increase from the sink and causes a bottleneck in the multihop packet flow. Compared to traditional sensor network where the usual bottleneck is near the sink [15], the bottleneck here is shifted towards the periphery of the network. In this research, we address this unique issue by effectively offloading some of the child's packet forwarding burden to the parent. We first compare the performance of transmitter-initiated versus receiver-initiated transmissions and show that the parent initiated process has a comparatively lower average delay, which is to the fact that the parent (in this case receiver) can take away some of the load from the children by initiating the transmission and reduce link delay of the child. Next, we allow a parent to further assist its child by optimally allocating its harvesting energy among transmission and reception activities, i.e., packet forwarding to the next parent and packet reception from its child. Extensive numerical results are presented to provide an insight into the upper bound characteristics of link throughput and optimal energy distribution strategy of the parent.

A summary of these key design considerations are illustrated in Fig. 1.3.

### 1.3 Organization of the Dissertation

The rest of the thesis is organized as follows. Chapter 2 discusses related works. In Chapter 3, we introduce cooperative relaying over unicast routes and propose an enhanced two-hop relaying protocol. The predictive retransmission strategy is discussed in Chapter 4. A load distribution method for RF energy harvesting networks is discussed in Chapter 5. We summarize our contributions in Chapter 6 followed by recommendations for future work.

## CHAPTER 2: RELATED WORK

Over the past decade, a large number of MAC [16–21] and routing [22–26] protocols have been proposed to efficiently deliver a packet from the source to the sink in multihop WSNs. However, most of these schemes are suitable for specific WSN scenarios and do a trade-off between energy budget, throughput, QoS, delay, and simplicity. In the first part of this chapter, we present a brief overview of the energy harvesting technologies. In the second part, we provide some of the MAC and routing layer protocols that are predominantly used in energy harvesting ICSNs for reducing the end-to-end transmission delay.

### 2.1 Energy Harvesting in Wireless Sensor Networks

Demand for long-lasting maintenance-free sensor network applications, the feasibility of deployment in potentially hazardous or sensitive monitoring applications, and scenarios with limited accessibility to nodes such as deeply embedded sensor networks have driven the research community to come up with alternate energy solutions to the onboard single-use batteries. In the recent years, tapping into the ambient energy sources such as solar, vibrations, thermal, etc. [6, 7, 27–30] as an alternative solution to the primary batteries has gained immense attention. In the following, we briefly discuss some of the popular energy sources used for powering sensor networks.

- **Photovoltaic:** Harnessing energy from the light sources by leveraging the photoelectric effect is one of the most mature technology for energy harvesting. It is simple, cheap, and easy way to convert ambient energy for the sensor devices because of the abundance of outdoor sunlight and adequate indoor lighting in many places. The amount of surface area for capturing light and illumination

level determine how much energy can be harvested. Typically it varies from 100 to 400  $mW$  for approximately 4 to 10  $inch^2$  surface area for harvesting (Helimote [31], Hydrowatch [32], SolarBiscuit [3], Prometheus [4]), which is pretty good compared to other energy sources. However, the complete unavailability of the solar source during the night and supply fluctuations due to the weather and season change require careful system design with sufficient storage capacity and long inoperability (for example, sleeping during the night). Also in many applications such as structural health monitoring and indoor sensing for smart homes etc., photovoltaic energy harvesting is not feasible due to the insufficient exposure to light.

- **Piezoelectric:** When external strain (usually through vibration or motion) is applied to the piezoelectric materials, it deforms their structure and generates potential. This energy can be generally harvested without the requirement of multistage processing to get necessary voltage levels. An extensive review of vibration energy harvest leveraging piezoelectric effect can be found here [29]. Vibrations generated from road traffic [9], factory machines [33], sound waves etc. are popular energy sources for piezoelectric harvesting. Furthermore, human motions such as footsteps [34,35] or push-buttons [36] are also explored as the source of energy. The amount of energy that can be harvested using piezoelectric effect is largely correlated to the energy source characteristics and the piezoelectric material properties. For instance, it can be observed in [9] that there is a noticeable spike in traffic-induced vibration energy harvesting whenever a vehicle crosses over the bridge. Typical harvest amount is 100  $\mu W/cm^3$  for vibration harvesters and 20 to 80  $mW$  peak power for footstep harvesters [7].
- **Thermoelectric:** In this type of harvesting, thermal energy is converted to elec-



tricity by utilizing the Seebeck effect. One end of the Thermoelectric generator has to be in contact with the heat source and the other end to a colder source. Some potential energy sources for thermal energy harvesting are human bodies [37, 38], room heater [39], CPU heatsinks [40] etc. The harvester characteristics are quite reliable and have long operational life, however, the harvesting efficiency is usually very low resulting in inadequate energy harvest (in the range of  $0.5 \mu W/mm^3$ ).

- Flow based: Airflow based harvesters typically deploy micro wind turbines to harvest energy from the wind flow through frequency voltage converters [41, 42]. However, the sensor node harvester combination is typically larger compared to other setups, and energy harvest amount greatly varies with the wind speed, direction, and obstructions. Another popular choice for flow-based harvesting is hydropower where the kinetic energy of the moving or falling liquid such as water is converted into the electricity [6]. Approximately  $20 mW$  constant energy supply can be obtained using a commercial harvester as shown in [43].

Besides the aforementioned harvesting techniques, the RF energy harvesting is gaining more momentum recently. Therefore, we mention the details of the RF energy harvesting schemes in a separate section in the following.

### 2.1.1 RF Energy Harvesting

RF energy harvesting is a process of harnessing energy from the far-field electromagnetic radiation in the RF band. Usually, this band ranges from 3 KHz to 300 GHz. However, most of the energy harvesting research activities are focused on TV [12], Cellular [44, 45], and ISM [46–48] bands. RF transmission (that may or may not contain information) is captured by the harvesting device’s antenna. In contrast to the regular radio receiver, however, here the energy receiving circuit has an RF to DC conversion channel for transferring incident energy at the antenna to a storage

device for energy accumulation. Capturing energy and information at the same time is also possible using power splitters or time-sharing mechanisms. This is known as simultaneous wireless power and information transfer (SWIPT) [49].

There are two types of RF energy sources [14], namely, i) ambient sources [44, 50]: these are already existing RF transmitters that are meant for domestic appliances such as TV, Bluetooth, WiFi, cellular transmissions, etc. and operates within 0.2 GHz to 2.4 GHz band, ii) dedicated sources [51, 52]: on-demand energy transmitters that usually operate in ISM bands with possibly narrow directional and high gain antennas. Usually, the received power density from ambient sources are extremely low but facilitates costless energy. On the other hand, dedicated energy sources can be leveraged for applications that have latency and throughput requirements.

In general, wireless energy transfer can be broadly categorized [8] into three groups—mechanical waves, magnetic fields, and electromagnetic radiations. RF energy harvesting falls under the larger category of electromagnetic radiations. A brief description of all three is provided below so that the reader can easily distinguish RF harvesting from the other two.

- Mechanical waves: mechanical waves propagate by generating oscillations (compression and expansion) in the media and transfer kinetic energy from one place to another. These oscillations cause vibrations in the receiving elements, thus facilitating vibrational energy harvesting. Among others, energy transfer via acoustic wave is the most commonly researched and easiest to implement technology. However, its efficiency and range are greatly affected by the propagation media.
- Magnetic fields: this method mainly utilizes magnetic fields and its electromagnetic phenomenon. Two transfer mechanisms are primarily used: inductive coupling and resonant inductive coupling. In inductive coupling, two magnetically coupled coils are deployed. By applying alternating current at the trans-

mitter coil, the magnetic field inside the coupled receiver coil can be changed, which generates the potential. This is suitable for near-field (in the cm scale) high-efficiency energy transfer applications. For inductive resonant coupling, a capacitance is added to each coil to form a tuned LC circuit. It is possible to attain high efficiency over a greater range relative to the coil's diameter by resonating both coils at a common frequency.

- Electromagnetic radiations: here energy carried in the electromagnetic waves are converted to electrical energy using antennas. Specialized antennas are included in both transmitter and receiver for high gain and narrow directivity. Energy can be steered towards various points using beam-forming, and transmitted up to several kilometers. In order to transfer energy more efficiently, low frequencies can be used for their lower path loss. However, lower frequencies require larger antennas which may not suit the smaller form factors of the network nodes. Furthermore, to avoid interfering other signals or minimize health hazards, government regulations restrict the transmission power. Therefore, careful design considerations for efficient energy transfer is necessary.

RF harvesting can be a great solution for future WSNs since, i) a large number of devices spread over a region can be easily powered ii) energy source and the harvester is spatially decoupled iii) energy can be harvested from the already existing ambient RF environment iv) harvested energy is usually stable, predictable and sometimes controllable. However, there are also some drawbacks such as i) very low harvest rate and high spatial correlation ii) energy reception sensitivity has to be higher compared to information reception iii) additional harvesting circuitry and power management is necessary.

## 2.2 Delay Minimization in Energy Harvesting ICSN

Reducing latency in ICSN is a challenging task due to the random outages in the sensor nodes. Protocols have to be designed in such a way that nodes can not rely on fixed transmission schedules or a fixed child-parent link. In this section, we discuss some of the existing MAC and routing layer solutions and their adoption into the energy harvesting ICSN.

### 2.2.1 MAC Layer Design

Medium access control dictates how and when a sensor node can access the shared wireless channel for transmission. Compared to the high throughput networks such as WiFi, contention for accessing the channel in WSN is quite low due to the energy constraint and application requirements. However, nodes in WSN periodically shut down their transceivers and go into the sleep mode to minimize energy consumption from idle listening. This poses a unique challenge for MAC since a successful data transmission can only take place when both the sender and receiver are awake. It becomes more challenging in energy harvesting ICSN where nodes not only go through the sleep and wake cycles but also a third state, the deep-sleep mode for energy harvesting. In the following, we first discuss the legacy MAC protocols that are popular in ICSN and how they minimize latency. Then we review some of the MAC protocols proposed specifically for energy harvesting sensor networks.

In contrast to synchronous MAC protocols such as S-MAC [53] where a small group of neighboring nodes, including the sender and the receiver, agree on the transmission schedule, asynchronous MAC does not require such mutual agreements, which makes it more suitable for ICSNs. A classic example of an asynchronous MAC protocol is B-MAC [54] where receiver nodes periodically wake up for a short period of time and sense the channel for ongoing transmission (see Fig. 2.1 (a)). This periodic channel sampling is known as low power listening (LPL). A potential transmitter

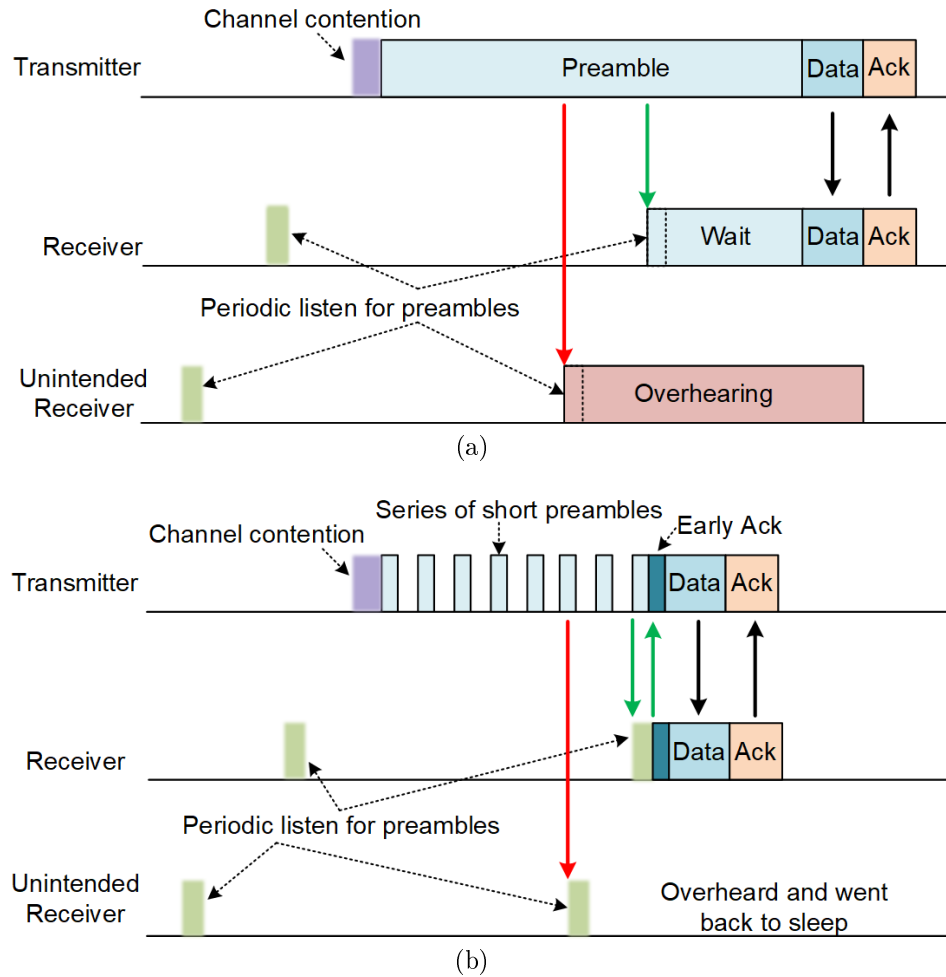


Figure 2.1: Operation of (a) B-MAC (b) X-MAC.

performs a clear channel assessment before transmission to avoid collisions. When the channel is free, it transmits a long preamble followed by the data packet and waits for the acknowledgment. The minimum length of the preamble is equal to the preamble sampling interval so that any receiver upon waking up can detect the transmission. After detecting the preamble, a receiver remains awake until the end of the transmission to receive the data packet. If the data packet is intended for itself, it immediately sends back an acknowledgment completing the whole packet delivery process. This process enables nodes to communicate with extremely low duty cycles, thereby conserving energy. A drawback is that a receiver has to wait

until the end of the transmission to receive a packet. Also, the unintended receivers have to keep listening until the end of the transmission to determine if the packet was destined for themselves. This causes overhearing in the unintended receivers, which causes wastage of energy. Furthermore, the channel remains occupied for the whole duration of preamble transmission producing an upper limit for the throughput performance. Nevertheless, due to the simplicity and popularity of B-MAC, it is often used as a baseline for newer protocol implementation. An improvement over B-MAC is proposed in X-MAC [55] where instead of sending a long preamble, a series of short preambles are strobed over the entire period. Here each preamble contains the address of the intended receiver so that a target node after receiving such a preamble can immediately ask for the data transmission. Also, any unintended receiver can go back to sleep as soon as they receive a short preamble (Fig. 2.1 (b)). This not only improves packet delivery delay but also reduces overhearing energy consumption in the neighbor nodes. BoX-MAC [56] and ContikiMAC [57] leverages the same idea. However, instead of sending the preamble bits, they incorporate data packets in the short preambles. This improves the delay performance by eliminating the additional time needed for the data packet request (through early acknowledgments in X-MAC) and transmission. These protocols, however, requires more computational resources since each short preamble is handled separately in layer 2. Another protocol, WiseMAC [58] improves delay performance by leveraging the neighbors wake-up schedules. Here nodes include their schedules in the data frames and acknowledgments. Any node receiving these transmissions build a local table according to the information. When a packet needs to be forwarded, the transmitter looks up in the table and tries to wake up exactly at the receivers wakeup schedule. To account for the clock drift a small preamble which is proportional to the time since the last schedule is updated is augmented before the data.

Receiver-initiated MAC protocols [59] added a new dimension to the MAC protocol

design. In all of the above-mentioned protocols, the sender initiates transmission by announcing its purpose in a preamble. This keeps the channel busy even when there is no actual data transmission going on. In comparison, in receiver-initiated MAC protocols, a sender that has data to transmit silently listens to the channel for potential receivers activity. Receiver nodes periodically wake up and broadcast a short beacon to let the sender know that it is ready to accept a packet. Upon reception of such a beacon from a target receiver, the sender responds immediately with a packet transmission. The receiver completes data forwarding process with an acknowledgment. The receiver goes back to sleep after a certain period of time if there is no data transmission. Receiver-initiated protocols reduce latency by occupying less channel resources and thus facilitating nearby nodes forward their packets. It also helps reducing overhearing since receivers listen to the channel only for a short duration. One of the earliest literature to propose receiver-initiated protocol is RICER [60] where in addition to the aforementioned scheme, a random delay between beacon reception and data transmission is introduced to minimize collisions. In [61] authors proposed RI-MAC which enables back to back data packet reception by incorporating a Ready-To-Receive (RTR) field in the acknowledgment. Since RI-MAC does not wait for a random delay after receiving a beacon similar to RICER, it introduces a collision resolution mechanism where receivers broadcast about collision events to inform senders.

MAC schemes specially designed for energy harvesting networks [21, 62] take the dynamics of the energy intake and consumption into the design consideration. A receiver-initiated MAC (OD-MAC) was proposed in [63] where nodes dynamically adjust their beacon transmission intervals and packet generation rates to achieve energy-neutral operation (ENO). Whenever there is an excess of energy in comparison to a predetermined optimal level, nodes either decrease the beacon interval (which reduces latency) or increases the packet generation rate (which increases throughput).

A probability threshold helps to decide among the two. Whenever there is a shortage of energy, nodes perform the opposite operation to reduce energy consumption. Another receiver initiated MAC was proposed in [64]. Here, nodes aggregate smaller packets into a larger one to reduce beacon sampling overhead. Also, it queues packets for a convenient duration by dynamically changing the timeout period so that the harvest rate stays below the consumption rate. Conventional MAC protocols such as TDMA and framed-ALOHA under the canvas of energy harvesting was analyzed in [65]. Authors of [66] proposed a probabilistic polling based MAC for single hop network where sink broadcasts a contention parameter. A potential sender that has harvested sufficient energy generates a random number. If the number is less than the broadcasted contention parameter, it initiates a transmission. Sink dynamically adjusts the contention parameter so that the likelihood of more than one node initiating a transmission is minimized.

These MAC protocols minimize latency by leveraging different properties of WSN. For our case, however, we mostly use B-MAC as a baseline to develop our new protocols.

#### 2.2.1.1 MAC Layer Design in RF Energy Harvesting Networks

In recent years, RF energy harvesting for powering small wireless devices is gaining substantial momentum among the research community [8, 13, 14, 67, 68]. Compared to other energy sources, RF sources are ubiquitous, often controllable, and easy to deploy. Design of the MAC layer for RF energy harvesting networks [69] mostly depends on whether or not there are dedicated energy sources present since harvesting is highly spatially correlated and a dedicated energy source provides some means for controlling the harvest rate. In this section, we go through some of the MAC protocols proposed in the recent literature for such networks.

A dedicated energy source based MAC protocol was proposed in [70]. Here nodes broadcast energy requests to nearby energy transmitters. Requesting node then cat-



egorizes the transmitters based on their phase differences and assigns different peak transmission frequencies so that the transmissions within same frequency contribute constructively to the level of RF energy received at the node. The protocol also dictates when energy requests are sent and how long energy is harvested so that energy transmission has less interference with overall data transmission. The underlying channel access mechanism is very similar to CSMA/CA, however, authors have used different slot duration, DIFS, and SIFS periods for energy and data transfer instances. Also, the back-off window for data transmission was dynamically adjusted so that nodes with higher energy residue get earlier access to the channel. A very similar method was proposed and evaluated in [71]. Another CSMA/CA based MAC protocol is proposed in [72]. Authors tried to achieve fairness by adjusting the contention window with a weighting factor. In contrast to the previous RF-MAC protocol, This weighting factor prioritizes nodes with less energy harvesting rate to transmit first. Also once a node reaches a fixed number of back off tries, it goes to sleep. Authors in [73] proposed an energy storage leakage aware duty cycling protocol to optimize energy-neutral operation. They applied linear quadratic tracking to regulate the active (therefore transmit and receive) and sleep times so that harvested energy level doesn't go up high which is good for leakage or don't go below a certain threshold. In [74], authors presented a polling based MAC for data forwarding. Here the sink node periodically broadcasts commands such as data transmission or synchronization for nodes to act upon. It also includes a timer counter to indicate when the action requested in the command should be performed. Before issuing this commands, sink node sends out energy signals to recharge the nodes. Due to spatial variance, channel characteristics and traffic demands, all node harvest at a different rate and may or may not capture these commands. Nodes that receive the commands set up a countdown timer. When the timer expires they randomly choose a slot to perform the action. However, before transmitting data packets, it senses the channel to avoid

a collision. If there are already transmission present in the channel, it simply drops the packet.

Many of the aforementioned schemes may not be suitable for ICSN due to their CSMA/CA based approach. Also requesting energy from RF transmitter is not always practical in a multi-hop scenario. In this research, we design an asynchronous MAC protocol for multi-hop scenario where parents assist their children by helping in packet forwarding process. We do this by decoupling the transmission and reception process and optimally adjusting the energy consumed for each activity. A detail of the protocol is discussed in chapter 5.

### 2.2.2 Routing Layer Design

Researchers have taken mainly two routing approaches to tackle packet forwarding in ICSN. The first one is opportunistic routing and other is unicast routing with cooperative relaying. In opportunistic routing, nodes are assumed to be aware of their geographic locations or hop distances from the sink. Any node within a chosen *forwarder set* that has the potential to forward the packet closer to the sink forwards it to the next hop. This type of routing opportunistically utilizes available energy in the surrounding nodes. Opportunistic routing has minimal control over the chosen route since there is no way to determine which node in the set is going to be the next-hop. For instance, in the illustration in Fig. 2.2(a), a packet transmitted by the source may be forwarded by one or more of nodes 2 – 8 that comprise the forwarder set of the source. Multiple methods have been proposed to choose this forwarder set. For instance, the authors of [75] considered the nodes within a  $[-30, 30]$  degree angle from the straight line connecting the source to the sink to be the forwarding set. The node within the forwarder set that first receives the packet acknowledges and forwards the packet to the next hop (node 5 in the example). In [76], the authors proposed an opportunistic routing scheme that leverages adaptive duty cycling to find the most eligible forwarder. Here, nodes that have higher energy go through more

frequent duty cycling. During a packet transmission, this increases the likelihood of getting a response from a candidate forwarder with higher energy. In contrast, our opportunistic routing scheme tries to minimize the number of failed attempts to find the first forwarder before it is selected. Author of [77] suggested a forwarding metric that is based on the neighbors energy parameters, the forwarder's harvesting rate, and duty cycles. Though this partially considers the energy availability of a route, it has a requirement of getting frequent neighbor information which is not quite feasible for an intermittently connected network. An opportunistic routing based on the remaining energy and channel state was proposed in [28]. Nodes with higher energy and better channel state (which are usually ones located close by) get the priority to become the forwarder. One of the concerns with this scheme is that more than one node in the forwarder set may receive the packet, which may result in multiple copies of the same packet to be forwarded to the sink. This might eventually lead to degraded communication performance in the network due to energy wastage, especially in ICSNs where energy is at a premium. Several approaches have been proposed to overcome this issue. Authors in [78, 79] split the forwarder set into a number of regions and assigned a priority to each region based on their potential routing progress. When multiple nodes in the forwarder set receive the packet, nodes from the highest priority regions declare themselves as next-hops first. Nodes from the lower priority zone discard the packet if they see that a node from a higher priority zone has already declared itself as the next-hop. However, even with this, the likelihood of forwarding multiple copies is not completely eliminated, since each priority region may consist of multiple nodes. Another approach presented in [80] requires immediate packet retransmission to inform the forwarding nodes that more than one node have received the packet.

Cooperative relaying over an unicast route is illustrated in Fig. 2.2(b). Here, every node determines the next hop through some unicast routing protocol, such as

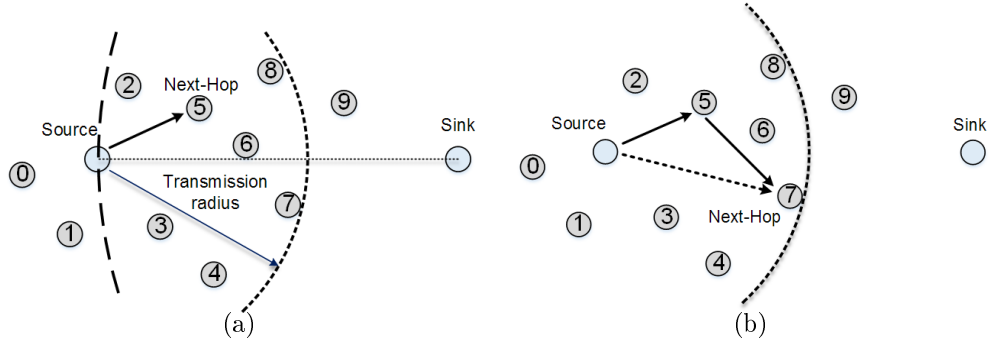


Figure 2.2: Operation of (a) opportunistic routing and (b) unicast routing with cooperative relaying in an intermittently connected network.

least cost routing. In Fig. 2.2(b), node 7 is the first hop from the source. When the source transmits a packet destined for node 7, neighbors that are common to both the source and node 7, such as node 5, assist in reducing the delay through cooperative relaying. In this scenario, if the source's transmission fails to reach 7 but is overheard by 5 (we call it the *relay* node), node 5 will independently try to forward the packet on behalf of the source. This improves the probability of reaching the destination earlier thereby reducing the transmission delay from the source to node 7. An automatic repeat request (ARQ) protocol based cooperative relaying scheme is presented in [81] to balance the energy among the neighbor nodes and increase overall throughput. A probabilistic retransmission scheme was proposed in [82] where optimal number of retransmissions were computed based on charge discharge time and number of potential forwarders. Authors in [83] presented optimal retransmission selection leveraging power control and energy harvesting rate. Often cooperative relaying is considered under the umbrella of MAC protocols. In HES-MAC [84], if a source does not receive CTS within three trials, it requests cooperation from one hop neighbors called bridge nodes. In case the destination is out of reach or has quite different sleep schedule, bridge nodes can help by diversifying the transmission attempts. In OC-MAC [85] when sources requests for cooperation (inserting current

energy level), potential neighbors cooperate if they see that their residual energy level is higher than the requesting source.

Opportunistic routing and cooperative relaying have their individual benefits. Under similar characteristics of intermittent connectivity, opportunistic routing typically provides lower average transmission delay by invoking higher node diversity. However, cooperative relaying provides several advantages that are beneficial in energy harvesting sensor networks. First, since cooperative relaying leverages unicast routing, packet duplication is minimized. Therefore, it does not require any additional mechanisms to reduce packet duplications. Next, unicast routing with cooperative relaying allows for more supervised and controlled routing. For example, in the illustration in Fig. 2.2(b), the source may choose node 1 as the next-hop to steer packets around node 2 – 8 if it observes that nodes 2 – 8 are getting congested or constrained in energy resources. While the relative performance of cooperative and opportunistic schemes are subject to successful implementations of energy conserving strategies and network topologies, here, our focus is on improving delay performance of each respective scheme through the application of predictive retransmission which is discussed in more detail in Chapter 4.

## CHAPTER 3: MINIMIZING DELAY USING TIME DIVERSITY

In this chapter, we address the problem of reducing multihop transmission delay in severely energy constrained ICSNs using *cooperative relaying over unicast routes*. To understand the underlying mechanism of cooperative relaying, let's consider the different system states (see Fig. 3.1 (a)) nodes go through in the energy harvesting ICSN. Whenever a node harvests energy up to a certain predefined threshold level, it transitions from the inactive harvest state to the active transmit or listen state. If it has a packet to forward, it transmits the packet immediately. The active duration of transmitter nodes are short and mainly comprised of preamble and data transmission. All other nodes after becoming active, periodically sleep and listen to the channel for transmitter activity. If they detect a preamble, they remain awake until the end of the preamble transmission to receive the data. Once their energy is depleted from continuous duty-cycling, they go back to the inactive harvest mode. A simple scenario where nodes become active right after harvesting enough energy to transmit a packet is illustrated in Fig. 3.1 (b). Since nodes have random active and inactive cycles, the time diversity of the neighbor nodes can be leveraged to spread the transmission attempts of the sender. This is described in Fig. 3.2. When a node's transmission attempt fails to reach the desired destination and a common neighbor (neighbor to both source and destination node) overhears the packet, it offers to cooperate by independently forwarding the packet on behalf of the source node. It is more likely that the packet will be delivered faster if more than one node attempt to forward it. Cooperative relaying improves energy utilization and minimizes delay by tapping into the energy resources of idle nodes in the vicinity of the source and destination, some of which would otherwise be wasted due to ambient processes such as overhearing or

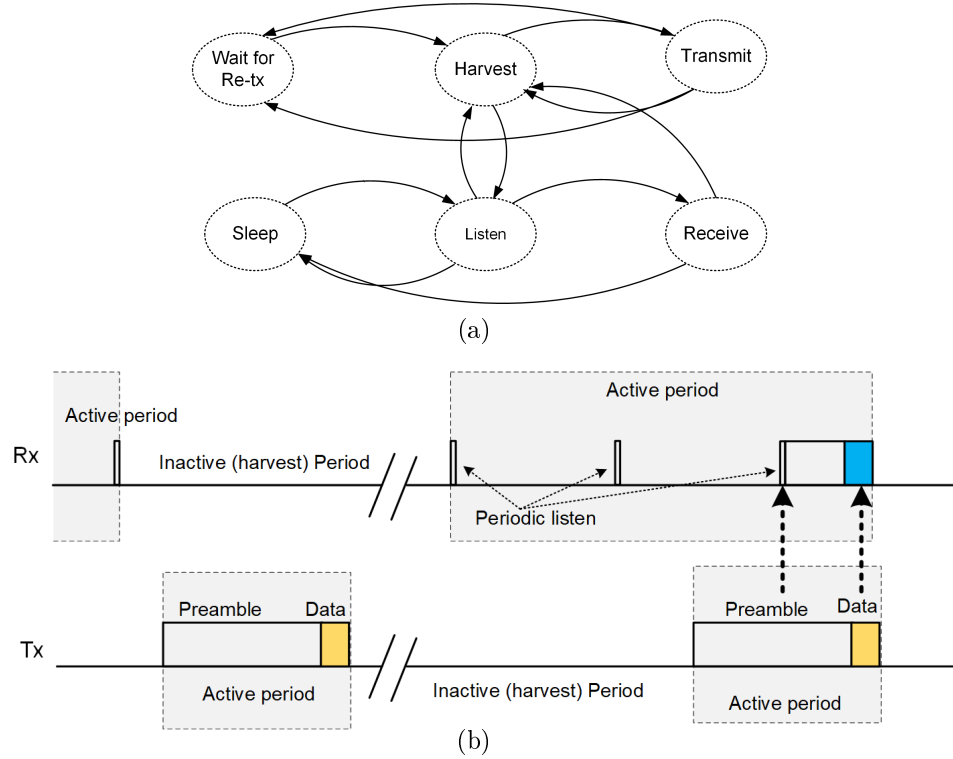


Figure 3.1: (a) System states of a node (b) how transmitter and receiver communicate while going through different states.

leakage. However, it also increases radio activity in the vicinity, leading to increased overhearing probability, and faster depletion of energy resources. In this chapter, we formulate and analyze the delay performance of the cooperative relaying scheme, and then propose a two-hop cooperation strategy for a more practical multi-hop network setup.

### 3.1 Analysis of Delay with Cooperative Relaying

In this section, we analyze the benefits of using cooperative relaying on reducing the transmission delay over an intermittently connected link. We formulate a mathematical model and present numerical results obtained from this.

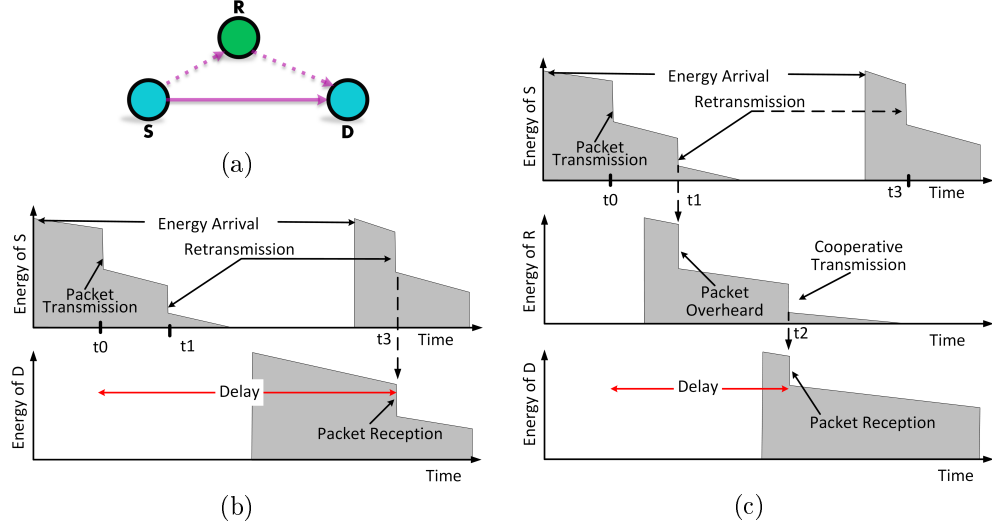


Figure 3.2: Illustration of the reduction of transmission delay in ICSNs using neighbor cooperation. (a) Sample scenario where source  $S$  has a packet to transmit to  $D$ . Node  $R$  is a potential cooperator that is in the range of both  $S$  and  $D$ . (b) Variation of energy resources at  $S$  and  $D$  during transmission without cooperation: when  $S$  transmits at  $t_0$  and  $t_1$ ,  $D$  does not have enough energy; transmission is eventually successful at  $t_3$ , resulting in a large delay (c) Corresponding energy variations at  $S$ ,  $D$ , and  $R$  when cooperation of  $R$  is applied:  $S$ 's transmission is overheard by  $R$  at  $t_1$ , which then starts relaying  $S$ 's packet and able to reach  $D$  at  $t_2$ , which is earlier.

### 3.1.1 Preliminaries

We consider event monitoring applications, where nodes periodically sample sensor data and report information to the sink through multi hop routing only when specific events of interest are detected. Examples of such applications include environmental condition monitoring, industrial systems monitoring, intrusion detection [86], and fire disaster management [87], to name a few. It is assumed that at the setup phase of the network, nodes gather route related data and slowly update the route information through ‘hello’ messages thereafter. We assume that nodes harvest energy from relatively weak environmental energy sources such as mechanical vibrations that occur at independently distributed random instants. Nodes store the harvested energy in SCs, and spend it judiciously, giving priority to sensing and processing tasks. When



a node's available energy level exceeds a threshold, it activates its radio for transmissions, receptions, and cooperation. Nodes are not time synchronized, which is difficult to achieve in intermittently connected networks. We assume that the energy availability is not sufficient to keep the radio in active state all the time, resulting in intermittent connectivity of the associated wireless links. In case an event is to be reported, a node utilizes its next available active state to transmit the packet to reach its parent (next hop en-route to the sink). In an active state, a node engages in a limited number of retransmissions until it receives an acknowledgment from its immediate destination. A random access MAC is assumed with asynchronous duty cycling, such as Low Power Listening (LPL) [88], to conserve energy in its active state..

Though cooperative relaying has the potential of reducing the delay, as stated earlier, it also increases the average energy usage due to a higher number of "radio events", i.e. transmissions, receptions, and overhearing, leading to shorter average active periods of the nodes. This affects the link connectivity. The effect is exacerbated with increased number of Cooperator Relays (CR). Hence, our objective here is to first explore the effect of different system parameters on the delay performance in such networks. To achieve this, we formulate a mathematical model for analyzing the delay performance in a single hop with and without a CR, which is described in the following.

### 3.1.2 Analytical Model

We consider a single-hop transmission scenario that comprises a source  $S$ , a cooperator relay  $R$ , and a destination  $D$ , as illustrated in Fig. 3.2(a). This can be a part of a multi-hop route. Initially,  $S$  contains a data packet that needs to be forwarded to  $D$ . Each node stores its harvested energy in an energy buffer that has a capacity of  $E_{max}$ . The average *ambient energy consumption* in a node due to leakage, sensing, and processing is denoted by the variable  $E_a$ . We assume that energy arrivals at all

nodes occur at random times, which are bursty events typical of mechanical energy harvested on a roadside or bridge obtained from vibrations of passing vehicles. Since such events are largely memoryless, it is reasonable to assume that the inter-arrival times of energy arrival events are exponentially distributed. For modeling and analysis, we assume a discrete time version of the energy arrival model for which such inter-arrival times can be described by a Geometrical distribution with parameter  $P_e$ . This implies that in the discrete time model, the energy arrival process in each node can be modeled as a Bernoulli process with arrival probability  $P_e$ . The amount of energy in each harvest is represented by a constant  $E_h$ . For the sake of simplicity, we assume that time is slotted and the duration of the slot is sufficiently small so that only one radio event can take place in a slot.

In a larger network, any of the nodes in consideration might overhear transmissions from other nodes in their neighborhood. In ICSNs, all transmissions are dependent on the active periods of the nodes, which depend on energy availability. Since the active periods of different nodes are memoryless, we assume that transmissions from neighboring nodes causing overhearing are random and memoryless. In data collection networks, such as in environmental monitoring applications, the data packets at different nodes are also generated independently. Hence, we model the packet overhearing also by a Bernoulli process, with probability  $P_o$ .<sup>1</sup> However, since the ambient data traffic is low in event monitoring networks,  $P_o$  should be very low. We assume that the energy consumed by a node in overhearing, transmission, and reception of a packet are the same, represented by  $E_{rd}$ . This is reasonable, since most low-power radios have similar figures for these events. The probability of a radio event in a node is denoted by  $P_{rd}$ . Any radio event is assumed to take place at the beginning of a slot and the harvested energy is added to the energy storage at the end of the slot. All acknowledgments are assumed to consume negligible energy, and are sent promptly

---

<sup>1</sup>Note that in event monitoring networks, data traffic in different nodes may have some correlation, but we ignore that in this work for the sake of mathematical tractability.

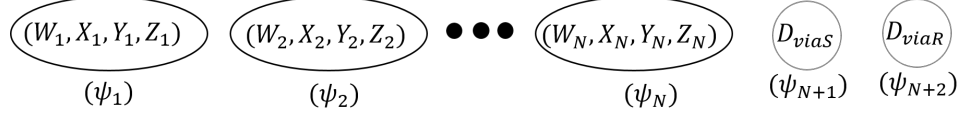


Figure 3.3: States of the Markov Chain.

after the reception. When a transmission is unsuccessful, it is repeated with a random delay. This is implemented using a transmissions probability  $P_{tx}$  for retransmission in each slot after an unsuccessful attempt.

With these assumptions, the three-node scenario can be modeled as a four-dimensional Discrete Time Markov Chain (DTMC), where the state is defined by the quadruple  $(w, x, y, z)$  as depicted in Fig. 3.3. Here  $w \in \{S, SR\}$  indicates whether only the source (denoted as  $S$ ), or both the source and relay (denoted as  $SR$ ) are currently holding a copy of the packet; and  $x, y$  or  $z \in \{m : m \in \mathbb{Z}_{\geq 0} \wedge m \leq E_{max}\}$  denotes the current energy levels of source, relay, and destination, respectively. The packet will be at the source initially, might be copied to the relay, and reach the destination eventually. Our objective is to find out the required time for the packet to reach the destination.

In order to simplify the analysis of this four dimensional system, we translate this four variables into a unique single variable  $i$  for ease of numerical computations. This is done by setting

$$\begin{aligned}
 i &= w \times (E_{max} + 1) \times (E_{max} + 1) \times (E_{max} + 1) \\
 &+ x \times (E_{max} + 1) \times (E_{max} + 1) \\
 &+ y \times (E_{max} + 1) + (z + 1)
 \end{aligned} \tag{3.1}$$

Here, we denote  $w = 0$  and  $1$  to represent the cases  $w = S$  and  $w = SR$ , respectively. This translation leads to  $N$  system states where  $N = 2 \cdot (E_{max} + 1) \cdot (E_{max} + 1) \cdot (E_{max} + 1)$ . These states are called transient states. In addition, there are two other states  $D_{viaS}$  and  $D_{viaR}$  that represent the state of the system when the destination

receives the packet, where the subscript indicates where the packet is received from. These two are absorbing states, i.e., when a system moves to any of these states, it will remain there forever.

We consider that whenever a packet is transmitted either by the source or a relay, and the destination is active, i.e., has sufficient energy to receive the packet, it will receive the packet immediately and the system will move from any of the transient states to the absorbing state. Now, the system will experience a transition if and only if any of the four variables in  $(w, x, y, z)$  changes within a time slot or the destination receives the packet. The values of  $x, y$  or  $z$  may change in four possible ways corresponding to various combinations of energy events and radio events in each node. To realize this, let's denote  $k \in \{x, y, z\}$  as the current value, and  $k'$  as the value after the transition. Then  $k'$ , and probability of transitioning into  $k'$  can be written as

$$k' = \begin{cases} \min(k - E_{rd} + E_{in}, E_{max}), & \text{with } P_{rd} \cdot P_e \\ \max(k - E_{rd} - E_a, 0), & \text{with } P_{rd} \cdot (1 - P_e) \\ \min(k + E_h, E_{max}), & \text{with } (1 - P_{rd}) \cdot P_e \\ \max(k - E_a, 0), & \text{with } (1 - P_{rd}) \cdot (1 - P_e) \\ \text{elsewhere,} & \text{with } 0 \end{cases} \quad (3.2)$$

To find the transition probabilities within the transient states, we first need to get  $P_{rd}$  and the possible values of  $w$  after transition. Since  $P_{rd}$  depends on whether the node has a copy of the packet, and how much energy it currently holds, each case must be considered separately. Let us assume that the radio event probability in the source, relay, and destination nodes are denoted by  $P_{rdX}$ ,  $P_{rdY}$  and  $P_{rdZ}$ , respectively, and the possible value of  $w$  after transition by  $w'$ .

If the current state is described by  $(w, x, y, z)$ , then the value of  $P_{rdX}$ ,  $P_{rdY}$ ,  $P_{rdZ}$  and  $w'$  can be found as follows:

Case 1:  $z \geq E_{rd}, x \geq E_{rd}$  and  $y < E_{rd}$

If  $w = S$  or  $w = SR$ , then  $w' = w$  with probability  $(1 - P_{tx})$ , and  $P_{rdX} = P_{rdZ} = P_o, P_{rdY} = 0$

Case 2:  $z \geq E_{rd}, x < E_{rd}$  and  $y \geq E_{rd}$

If  $w = S$ , then  $w' = w$  with probability 1, and  $P_{rdY} = P_{rdZ} = P_o, P_{rdX} = 0$

If  $w = SR$ , then  $w' = w$  with probability  $(1 - P_{tx})$ , and  $P_{rdY} = P_{rdZ} = P_o, P_{rdX} = 0$

Case 3:  $z \geq E_{rd}, x \geq E_{rd}$  and  $y \geq E_{rd}$

If  $w = S$ , then  $w' = w$  with probability  $(1 - P_{tx})$ , and  $P_{rdX} = P_{rdY} = P_{rdZ} = P_o$

If  $w = SR$ , then  $w' = w$  with probability  $(1 - P_{tx})^2$ , and  $P_{rdX} = P_{rdY} = P_{rdZ} = P_o$

Case 4:  $z \geq E_{rd}, x < E_{rd}$  and  $y < E_{rd}$

If  $w = S$  or  $w = SR$ , then  $w' = w$  with probability 1, and  $P_{rdX} = P_{rdY} = 0, P_{rdZ} = P_o$

Case 5:  $z < E_{rd}, x \geq E_{rd}$  and  $y < E_{rd}$

If  $w = S$ , then  $w' = w$  with probability 1, and  $P_{rdX} = P_{tx} + (1 - P_{tx}) \cdot P_o, P_{rdY} = 0, P_{rdZ} = 0$

If  $w = SR$ , then  $w' = w$  with probability 1, and  $P_{rdX} = P_{tx} + (1 - P_{tx}) \cdot P_o, P_{rdY} = 0, P_{rdZ} = 0$

Case 6:  $z < E_{rd}, x < E_{rd}$  and  $y \geq E_{rd}$

If  $w = S$ , then  $w' = w$  with probability 1, and  $P_{rdX} = P_{rdZ} = 0, P_{rdY} = P_o$

If  $w = SR$ , then  $w' = w$  with probability 1, and  $P_{rdY} = P_{tx} + (1 - P_{tx}) \cdot P_o, P_{rdX} = P_{rdZ} = 0$

Case 7:  $z < E_{rd}, x \geq E_{rd}$  and  $y \geq E_{rd}$

If  $w = S$ , then  $w' = S$  with probability  $1 - P_{tx}$ , along with  $P_{rdX} = P_{rdY} = P_o, P_{rdZ} = 0$ , and  $w' = SR$  with probability  $P_{tx}$  along with  $P_{rdX} = P_{rdY} = 1, P_{rdZ} = 0$

If  $w = SR$ , then  $w' = w$  with probability 1, and  $P_{rdX} = P_{rdY} = P_{tx}^2 + 2 \cdot (1 - P_{tx}) + (1 - P_{tx})^2 \cdot P_o, P_{rdZ} = 0$

When cooperation is not applied, potential cooperators should not retain a copy of the packet to forward on behalf of the source. That is, the system will never move

from  $w = S$  to  $w = SR$ . Under this situation,

If  $w = S$ , then  $w' = S$  with probability 1, and  $P_{rdX} = P_{tx} + (1 - P_{tx}) \cdot P_o, P_{rdZ} = 0$

Case 8:  $z < E_{rd}, x < E_{rd}$  and  $y < E_{rd}$

If  $w = S$  or  $w = SR$ , then  $w' = w$  with probability 1, and  $P_{rdX} = P_{rdY} = P_{rdZ} = 0$

With these, the probability of moving from a transient state  $S_i$  to  $S_j$  can be written as follows:

$$P_{i,j} = P_{w_i,w_j} \times P_{x_i,x_j} \times P_{y_i,y_j} \times P_{z_i,z_j} \quad (3.3)$$

where  $S_i$  can be decomposed into quadruple  $(w_i, x_i, y_i, z_i)$ , and  $S_j$  into  $(w_j, x_j, y_j, z_j)$ .  $P_{x_i,x_j}$  denotes the probability of moving from  $x_i$  to  $x_j$ . All the probabilities required for this equation can be found from Eq.3.2 and the cases described above.

We now construct the state transition matrix  $P$ , where the element  $P_{i,j}$  in  $i^{th}$  row and  $j^{th}$  column represents the state transition probability. We divide the state space of the DTMC into two subsets, one containing all the transient states, and another the two absorbing states. We can represent the transitions in  $P$  as,

$$P = \left[ \begin{array}{ccc|cc} P_{1,1} & P_{1,2} & \cdots & P_{1,N+2-1} & P_{1,N+2} \\ P_{2,1} & P_{2,2} & \cdots & P_{2,N+2-1} & P_{2,N+2} \\ \vdots & \vdots & \vdots & \vdots & \vdots \\ \hline 0 & 0 & \cdots & 1 & 0 \\ 0 & 0 & \cdots & 0 & 1 \end{array} \right] \quad (3.4)$$

If we denote the upper left partition of the matrix by  $T$ , the upper right by  $U$ , and the lower right by  $A$ , then we may express the matrix  $P$  by,

$$P = \left[ \begin{array}{c|c} T & U \\ \hline 0 & A \end{array} \right] \quad (3.5)$$

To find the expected delay before the packet gets delivered to the destination, it is

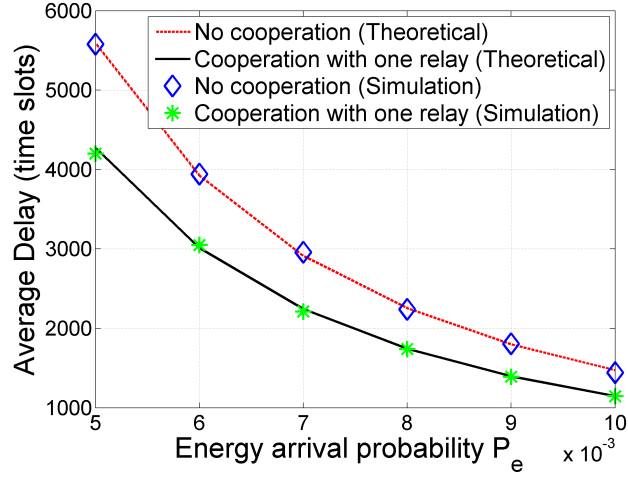


Figure 3.4: Comparison between theoretical model and simulation.

Table 3.1: Parameters used in the analysis for cooperative relaying.

Energy storage capacity, $E_{max}$	20
Energy consumed in a radio event, $E_{rd}$	10
Amount of energy in each harvest, $E_h$	20
Average ambient energy consumption, $E_a$	1
Probability of overhearing $P_o$	0.0001
Transmit probability in each slot, $P_{tx}$	0.1

necessary to find the expected time that the system spends before moving into any of the absorbing states. This can be found from the following equation [89],

$$D = (I - T)^{-1} \cdot e \quad (3.6)$$

where  $e$  is a column matrix of ones. Here, the  $i^{th}$  element of  $D$  provides the mean time to absorption from state  $i$ .

Numerical results obtained using this model on the average delay over a wireless link with and without cooperative relaying are plotted in Fig. 3.4. The figure depicts the variation of the average delay with  $P_e$ , where the overhearing probability  $P_o$  is fixed at 0.0001 per slot, and all other parameters as listed in Table 3.1. These results

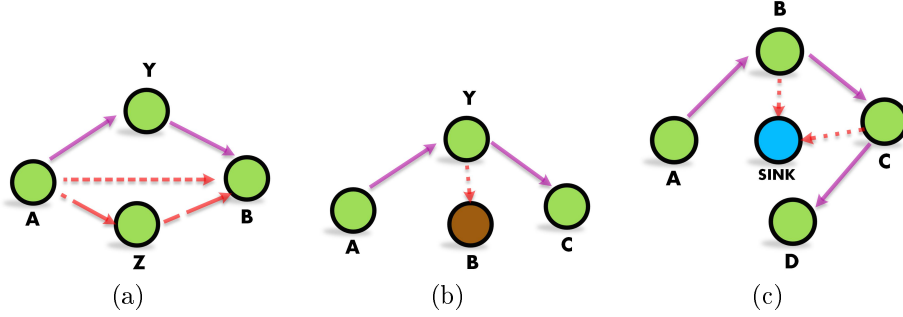


Figure 3.5: (a)Wasting next-hop parents energy, (b)deteriorating energy of two-hop parent, (c)energy wastage surrounding the sink node.

clearly depict that cooperative relaying reduces the average delay, which is due to transmission diversity. The delay improvement is particularly pronounced at low energy arrival rates, i.e. when the link connection is more intermittent. The theoretical results are validated with those obtained from computer simulations written in C++.

While these results are encouraging, it must be noted that these were obtained for a constant radio event probability. In reality, cooperative relaying will result in additional radio activity that will depend on the network scenario and event probabilities, and needs to be evaluated using a full scale network model.

### 3.2 Ephemeral Two-hop Opportunistic Cooperation (ETOC)

We next present the design of an *Ephemeral Two-hop Opportunistic Cooperation (ETOC)* protocol that applies cooperative transmissions in unicast routing along with some additional design considerations for minimizing the delay in a multi-hop network. The design principles of ETOC are described by considering the following issues that are addressed by ETOC.

- *Issue I: Source unaware of CR's success:* Consider the scenario in Fig. 3.5 (a), where A is trying to transmit a packet to B, but depletes its energy before it is successful. The CR node Y is successful in transmitting A's packet to B before A becomes active. When A becomes active again, it does not know that Y



was successful. So it keeps transmitting, wasting its own energy and that of its neighbors. It was observed that a key impact of this was the reduction of the energy of B, thereby reducing its chances of forwarding the packet to the next hop.

- *Issue II: CR unaware of success:* In addition to A, neighboring node Z could also be unaware of the successful transmission of the packet from Y to B, and wake up after the event and start relaying the same packet. This will waste its neighbors energy (including A and Y) through repeated transmissions.
- *Issue III: Up-stream node gets relayed packet first:* Next, assume that while node Y is trying to forward node A's packet to B (Fig. 3.5 (b)), an up-stream node C receives the packet, which is not received by B. This should be used for forwarding the packet without the participation of B, to conserve energy.

We take the above considerations into account in designing ETOC. First, in consideration of the issue I, we used a priority based channel access scheme similar to SIFS/DIFS in IEEE 802.11 DCF. An additional delay  $d_i$  is introduced to the  $i^{th}$  node that is proportional to the distance to the sink so that nodes in the routing path get more priority than the cooperator nodes for transmission. For example, once node B got the packet from Y (see Fig. 3.5 (a)), B will always get priority to access the channel before node Y, Z or A; hence it will be able to forward the packet faster. Although this does not solve the energy wastage problem described in Issue I, it still resolves the issue of reducing the delay in forwarding the packet along the route.

To overcome issue II, we introduce a Time to live (TTL) field in the data packet. This field is updated whenever the packet reaches any node except the cooperators in the routing path. TTL is set according to the expected time needed if this was a direct transmission. When a potential cooperator receives the packet, it keeps checking whether the packet's TTL is expired. If expired, the cooperator assumes that the

packet is already delivered to next parent and is discarded. These precautions are particularly useful when network traffic is high and the energy harvesting rate is low.

Finally, as described in the issue III above, a cooperator might be able to reach two hop parent during it's transmission. Therefore, in ETOC, whenever a cooperator sees that the two hop parent is in it's neighbors list, it directly acts as a cooperator for that parent. This enables a cooperator node to opportunistically expedite the progress of the packet along the route.

A possible problem that can arise with the two-hop relaying scheme is illustrated in Fig. 3.5 (c), where at the end of the routing path, i.e., near the sink, B becomes a cooperator for node A. However, B's transmission may be picked up by C and D, as both of them have the sink in their neighbor list. This will result in a large energy wastage around the sink. To address this problem, we set up another condition. If the potential cooperator's distance to sink is smaller than the source node, it will not be a cooperator. This ensures that the cooperators will not surround the sink.

### 3.3 Performance Results

To evaluate the performance of ETOC, simulations were performed using the multi-agent based programming tool *Netlogo* [90]. An energy harvesting sensor network was considered with 97 nodes arranged in a uniform grid (see Fig. 3.6), and a sink at the center of the network. The node separation was assumed to be 7 units, and the transmission range is assumed as 11 units. Alarm events were generated at exponentially distributed random intervals with sufficiently large mean (20000 units) to avoid packet buffer delays. For each alarm event, a random source was chosen that forwarded a data packet on the shortest path route with or without cooperation.

For MAC, a time slotted operation was considered. When a node wants to transmit, it evaluates its priority and assigns an associated delay (as discussed in the previous section) from the beginning of the slot before it can transmit. While waiting for the delay to expire, it keeps sensing the channel. If the channel gets busy, i.e., some other

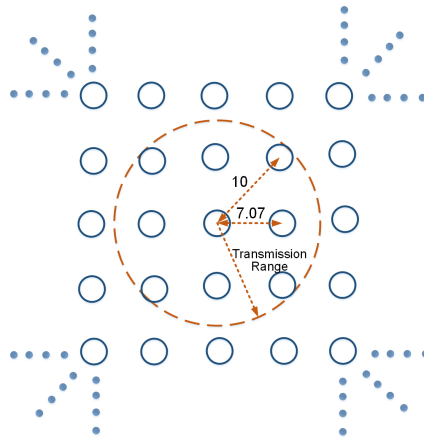


Figure 3.6: Network model used for simulation experiments.

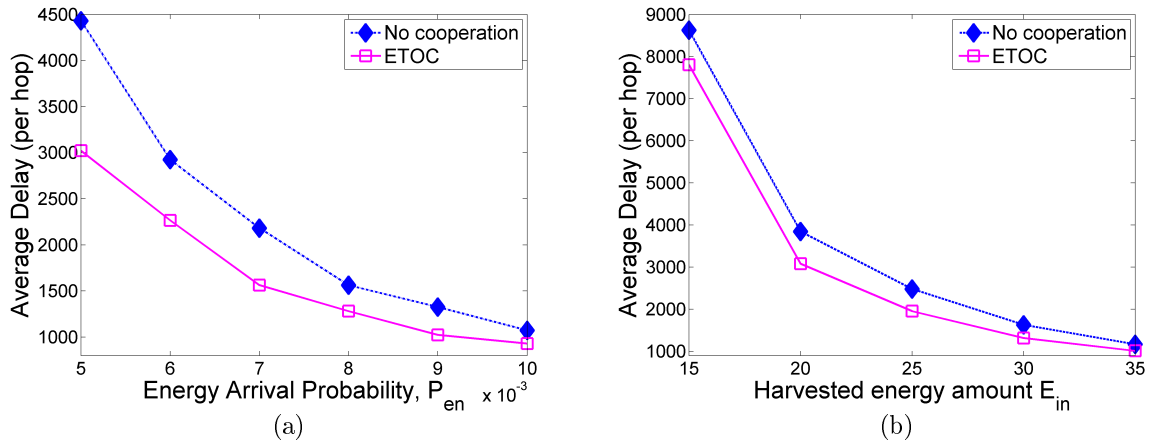


Figure 3.7: Delay improvement from cooperation.

node with higher priority started transmission, it aborts the delay countdown and goes to reception mode. Otherwise, it transmits after the delay expires. Since delay depends upon the geographic distance, the chances of collisions are negligible.

Simulation results presented in Fig. 3.7 suggests that up to 31.81% improvements in the end-to-end transmission delay were achieved through ETOC compared to direct transmission. The results indicate that the delay is very sensitive to energy harvesting rate and decreases exponentially with increasing values of harvested energy. This is expected, since the node outages become less frequent with increasing values of

energy harvesting. This is also consistent with our findings from section IV. Also, we note that improvement of the delay performance using ETOC is higher when the network connectivity is more intermittently, i.e., for lower energy arrival probabilities. It is interesting to note that for the same energy arrival rate, the performance improvement is relatively unaffected by  $E_{in}$ . To conclude, we demonstrate that the collective time diversity of the source and cooperative relays can improve the overall delay performance. However, we recognize that the delay performance can be further improved by enhancing individual node performance through a judicious choice of retransmission intervals which is discussed in the next chapter.

## CHAPTER 4: ACHIEVING LOW LATENCY THROUGH TRANSMISSION TIME ESTIMATION

To minimize transmission delay over intermittently connected links, we consider *optimizing the retransmission interval* in this chapter. The idea is to determine the best time for a retransmission attempt after each failed transmission that maximizes the probability of successfully reaching a destination. It is well known that transmission and reception events are the biggest consumers of the energy [91–93] in low power wireless sensor nodes. Each energy harvesting phase enables the source to attempt only a limited number of transmissions to forward the packet to its parent node. Therefore, to avoid long harvesting phases, each attempt should be as much effective as possible. When energy arrival events are infrequent, interspacing between retransmissions should be based on the destination node’s harvested energy, and the source and destination’s energy consumption rates to improve the probability of success. If the retransmission interval is too small, it will result in high energy wastage due to many unsuccessful retransmissions. On the other hand, an excessively high retransmission interval might result in missing the window of time when the receiver becomes active and result in a longer average delay. We first develop the basis for the probabilistic predictive retransmission scheme and then apply this to two different transmission diversity schemes, cooperative relaying over unicast routes and opportunistic routing to further reduce the delay.

### 4.1 Predictive Retransmission for Intermittent Wireless Links

In this section, we first demonstrate that the probability of success in an intermittently connected wireless link can be maximized by the selection of an optimum

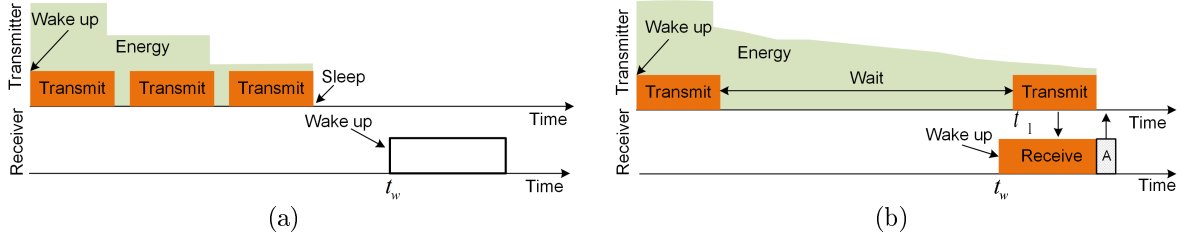


Figure 4.1: Illustration of (a) back-to-back and (b) predictive retransmissions.

retransmission interval that depends on the available energy level at the node, energy harvest and consumption rate. We then show that using the optimum retransmission interval for every retransmission attempt minimizes the average packet transmission delay over the intermittently connected wireless link. The idea is illustrated in Fig. 4.1. In Fig. 4.1 (a), the transmitter employs back-to-back retransmissions, where the expectation is for the receiver to receive and acknowledge the packet whenever it wakes up. However, as illustrated in Fig. 4.1(a), this might lead to a situation where the transmitter depletes its energy before it reaches the receiver. We propose that instead of performing immediate retransmissions, it is more effective for the transmitter to retransmit at a time *when the probability of the receiver waking up is predicted to be maximum* (see Fig. 4.1(b)). This reduces wasteful retransmissions and maximizes the probability of successful transmission in the transmitter's current active period, thereby reducing the risk of the transmitter going back to sleep prior to successfully transmitting the packet.

#### 4.1.1 Energy Dynamics of a Sensor Node

In order to predict the optimal retransmission time, it is essential to characterize the energy dynamics of a sensor node. The basic energy expenditure and harvesting behavior of a node is the same as described in chapter 3. Based on these assumptions, we can conclude that the energy stored in a sensor node's storage device changes due to primarily three causes:

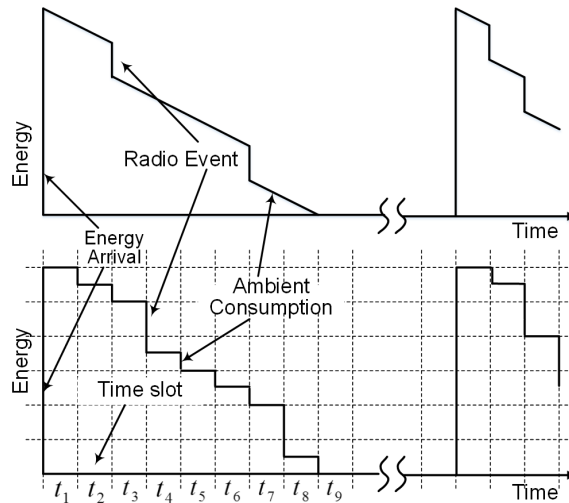


Figure 4.2: Continuous time representation (top) and its discrete time approximation (bottom) of the variation of energy level in a rechargeable sensor node.

- First, the energy level increases by  $E_h$  for each “energy arrival” event as discussed previously.
- Second, the energy gets depleted due to radio events, which includes packet transmissions (consumes  $E_t$ ), receptions (consumes  $E_r$ ), or overhearing (consumes  $E_o$ ).
- Finally, we consider that when a node is in active state, ambient events such as sensing, processing, and low power listening depletes its energy at a constant rate. To simplify, we term all these activities together as “ambient-activities”, which require an average “ambient consumption” of  $E_a^t$  or  $E_a^{nt}$  energy for transmitter and non-transmitter respectively. This spans throughout the active period.

Variations in a node’s energy level due to these activities are illustrated in the top of Fig. 4.2. When the energy is depleted to such a level that a node can no longer participate in transmissions or receptions, it goes into a deep-sleep or *inactive mode*. Due to low and random energy availability, the length of the inactive period is

Table 4.1: Notations used

$E_h$	Amount of energy in each harvest
$E_c$	Energy remaining in the storage
$E_t$	Required energy for a packet transmission
$E_r$	Required energy for a packet reception
$E_o$	Energy consumed in overhearing
$E_a^t$	Ambient consumption by transmitting node
$E_a$	Ambient consumption of a general node
$P_e$	Energy arrival probability
$P_o$	Probability of overhearing
$P_c$	Probability that the channel is error free
$T_w$	Waiting time before retransmission

assumed to be large compared to the active periods and no node can schedule sleep wake cycles ahead of time.

To make computations tractable, we consider a discrete time version of this continuous time model (bottom of Fig. 4.2). We assume that time is slotted and each slot is sufficiently small so that only one transmission can take place in a slot. The interval between two successive energy arrival events can then be represented by a Geometric distribution with a parameter  $P_e$ . Considering that the energy arrival rate is small, i.e. the inter energy arrival times are long, the probability of occurrence of another energy arrival event while a node is still active is negligible. For simplification, we assume that all energy related events, such as harvesting and consumption, occur at the end of the time slot. Since all nodes perform LPL, any node can capture the transmission of a nearby node as long as it is active. This is described as overhearing (having a probability parameter  $P_o$ ). With these considerations, we formulate the optimal waiting time before retransmission in the following section. A summary of the notations used is presented in Table 4.1.



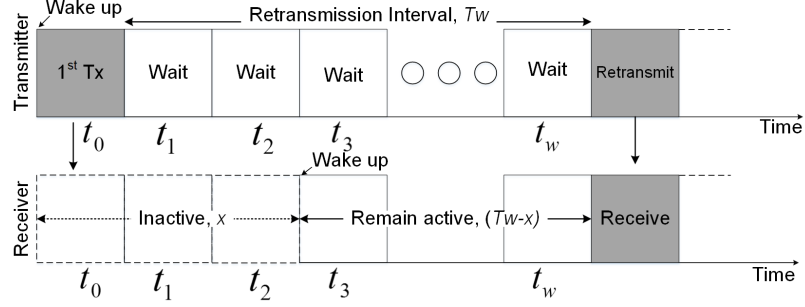


Figure 4.3: Finding the optimal retransmission interval.

#### 4.1.2 Optimal Retransmission Interval

Once a transmission is unsuccessful (due to the fact that the destination is inactive), a successful rendezvous between active states of a transmitter and receiver requires that the transmitter remains active while the destination wakes up from the sleep state and remains reception-capable (i.e. has sufficient energy to receive) for at least up to the point where the transmitter retransmits. In the following, we develop each of these probabilities for the back-to-back transmissions and that using a retransmission interval of  $T_w$  after a failed transmission attempt.

**Probability that transmitter remains active:** To find the success probability of a retransmission at a random time, we first find the probability that the source *remains active up to that time*. Let's consider Fig. 4.3, where a transmitter node wakes up from the inactive state at  $t_0$  with  $E_h$  amount of energy. After waking up, it immediately performs a transmission, which is unsuccessful. The transmitter node is now left with  $E_c = E_h - E_t$  amount of energy. If the node decides to wait for an interval  $T_w$  before the next retransmission, it has to have at least  $E_c - E_t$  energy by the end of  $T_w$  waiting period to perform another transmission. Now, if the transmitter overhears  $\eta$  packets within  $T_w$ , the following inequality must hold in order for it to

be able to retransmit at  $(T_w + 1)$

$$\begin{aligned} \eta E_o + (T_w - \eta) E_a^t &\leq (E_c - E_t) \\ \text{or, } \eta &\leq \frac{(E_c - E_t) - T_w E_a^t}{(E_o - E_a^t)} \end{aligned} \quad (4.1)$$

The maximum amount of overhearing that it will be able withstand and still remain capable of retransmission is

$$\eta_m^t = \left\lfloor \frac{(E_c - E_t) - T_w E_a^t}{(E_o - E_a^t)} \right\rfloor \quad (4.2)$$

Now, the probability of remaining capable of transmission after  $T_w$  is given by the probability of overhearing at most  $\eta_m^t$  packets within  $T_w$ , which is

$$P_w^t(T_w) = \sum_{i=0}^{\eta_m^t} \binom{T_w}{i} P_o^i (1 - P_o)^{T_w - i} \quad (4.3)$$

**Probability that receiver is active:** In order for the retransmission to be successful, it is also required that the receiver *wakes up in the mean time, and remains capable of reception* until the time of retransmission. The probability that the receiver wakes up after  $x$  (see Fig. 4.3) is  $P_e(1 - P_e)^{(x-1)}$ . After waking up, the probability that it remains capable of reception from  $x$  to  $T_w + 1$  and beyond can be expressed as

$$P_w^r(T_w + 1 - x) = \sum_{i=0}^{\eta_m^r} \binom{T_w + 1 - x}{i} P_o^i (1 - P_o)^{T_w + 1 - x - i} \quad (4.4)$$

where

$$\eta_m^r = \left\lfloor \frac{(E_h - E_r) - (T_w + 1 - x) E_a^{nt}}{(E_o - E_a^{nt})} \right\rfloor \quad (4.5)$$

#### 4.1.2.1 Probability of Success with Predictive Retransmission Interval

The probability of a successful retransmission after an interval  $T_w$  is then given by the product of the probabilities of the source remaining capable of transmission up to that time and that the receiver wakes up prior to  $T_w$  and remains capable of reception afterwards. In summary, the probability of a successful retransmission is obtained as

$$P_w^s(T_w) = P_w^t(T_w) \sum_{x=1}^{T_w+1} [P_e(1 - P_e)^{(x-1)} P_w^r(T_w + 1 - x)] P_c \quad (4.6)$$

Therefore, the maximum success probability achievable with the next retransmission is

$$P_m^p = \max_{T_w} P_w^s(T_w) \quad s.t. \quad 0 \leq T_w \leq \left\lfloor \frac{(E_c - E_t)}{E_a^t} \right\rfloor \quad (4.7)$$

Consequently, the optimum retransmission interval that maximizes the probability of a successful retransmission is given by

$$T_o^p = \arg \max_{T_w} P_w^s(T_w) \quad (4.8)$$

The optimum solution  $T_o^p$  depends on the parameters listed in Table II, which include fixed parameters as well node-specific and environmental parameters. While the fixed parameters depend on the hardware platform used, node-specific parameters such as the energy arrival and overhearing probabilities, the amount of energy in each harvest, and the current energy level may be estimated by the nodes. To avoid extensive computations, each node may obtain  $T_o^p$  from look-up tables that are computed offline based on a select set of fixed parameters and a range of node-specific dynamic parameters. Note that this requires mostly static parameters and a small number of dynamic parameters, most notably the current energy level.

To determine the effect of different node parameters on the optimum retransmission interval, we plot the variations of the probability of successful retransmission with a

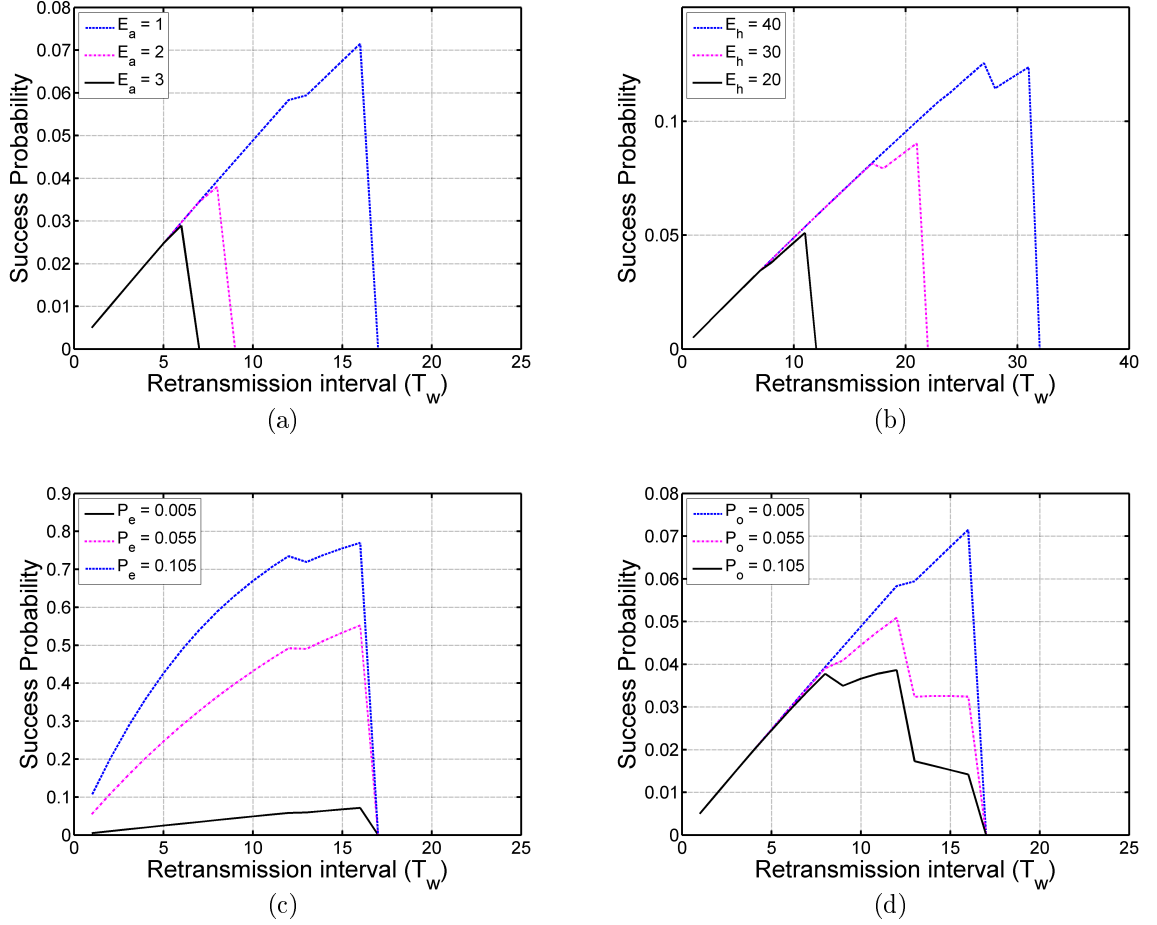


Figure 4.4: Probability of success of packet retransmissions in an intermittently connected wireless link using different retransmission intervals. In (a)  $P_e = 0.005$ ,  $P_o = 0.005$ ,  $E_h = 25$  in (b)  $P_e = 0.005$ ,  $P_o = 0.005$ ,  $E_h = 25$  in (c)  $P_o = 0.005$ ,  $E_a = 1$ ,  $E_h = 25$  in (d)  $P_e = 0.005$ ,  $E_a = 1$ ,  $E_h = 25$ .

retransmission interval  $T_w$  for different sets of parameters in Fig. 4.4. The default parameters for these figures are provided in Table 4.2. Also, since the energy arrival probability is quite low, we approximate the Binomial distributions of (4.3) and (4.4) with a Poisson distribution. We also consider  $P_c = 1$  to focus mainly on parameters related to the sensor nodes.

In Fig. 4.4 (a) we study the effect of the ambient energy consumption on the optimal retransmission interval. It is observed that the probability of success for retransmissions generally increases with increasing values of  $T_w$ . This is due to the

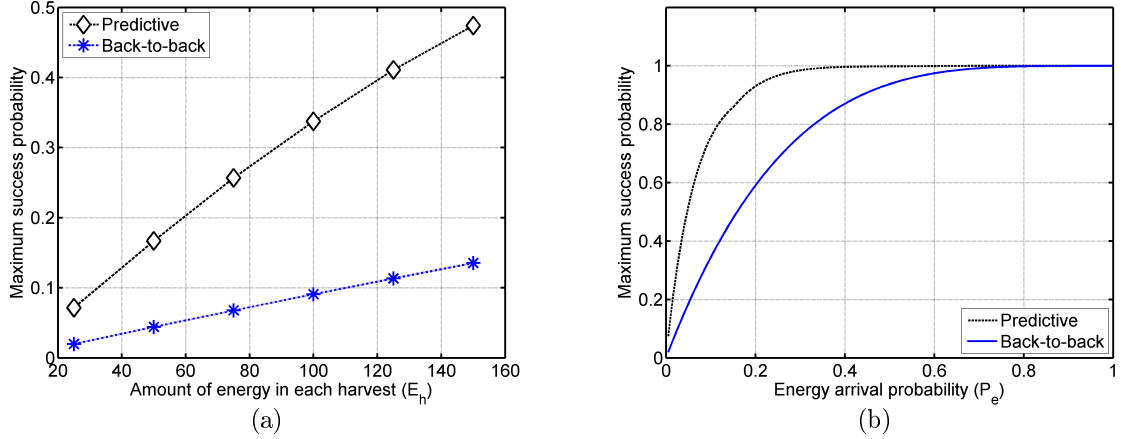


Figure 4.5: Maximum success probability achievable using predictive and back-to-back retransmissions in an intermittently connected wireless link.

Table 4.2: Node Parameters

Amount of energy in each harvest, $E_h$	25
Required energy for a radio event, $E_r$	5
Energy consumption from ambient activities, $E_a$	1
Probability of an error free channel, $P_c$	1
Probability of overhearing, $P_o$	0.005
Energy arrival probability, $P_e$	0.005

fact that a longer interval allows more likelihood of the receiver becoming active in the meantime. However, if the retransmission interval becomes too long, the success probability sharply falls since the transmitter loses energy from ambient activities. It must be noted that when the ambient energy consumption is high, the probability of success is lower. Fig. 4.4 (b) suggests a smaller waiting period between successive retransmissions if harvested energy is low.

A general observation from these two figures is that the probability of success is highest for the longest possible retransmission interval, i.e., it is better to wait until only enough energy for a single transmission is left. For example, if we assume that a node currently has 20 units of energy, each radio events consumes 5 units of energy,

and ambient activities constantly consume 1 unit of energy, the node should wait for 15 time units before the next retransmission. This maximizes the chances for the receiver to become active while the source still has energy to transmit. However, this observation does not apply for all the cases. For example, Fig. 4.4 (b) depicts that for  $E_h = 40$ , the optimal waiting time becomes 27 instead of 30. In Fig. 4.4 (c), we see the variations of the optimal retransmission interval with respect to different energy arrival probabilities. Here, small increase in energy arrival probability has little effect on the optimal delay time, however, the success probability is vastly improved. This is due to the fact that a higher waiting time ensures a higher likelihood of the receiver becoming active regardless of the energy arrival probability. Fig. 4.4 (d) indicates that the success probability significantly decreases with higher  $P_o$ , which indicates the detrimental effect of higher overhearing.

#### 4.1.2.2 Probability of Success with Back-to-back Retransmissions

To perform a comparison, we now obtain the maximum success probability associated with back-to-back retransmissions. Given that and the first transmission is not successful, if the maximum number of transmission attempts possible after waking up from inactive state with  $E_h$  energy is denoted by  $\beta + 1$ , then we can write

$$\beta = \left\lfloor \frac{(E_h - E_t)}{E_t} \right\rfloor \quad (4.9)$$

Here, the success probability for each retransmission attempt depends on whether the receiver underwent an energy arrival event in the previous slot and also on the channel condition. The cumulative success probability for retransmissions can therefore be written as

$$P_m^b = \sum_{i=1}^{\beta} P_e P_c (1 - P_e P_c)^{i-1} \quad (4.10)$$

We plot the maximum attainable success probability using back-to-back retransmissions and that using the proposed predictive retransmission scheme in Fig. 4.5. It

is clear that the predictive retransmission strategy offers higher probability of success compared to back-to-back transmission policy by leveraging the statistical information at the time of the first transmission and adjusting the retransmission interval accordingly. Moreover, the back-to-back retransmission is a special case for the predictive retransmission scheme when  $T_w = 0$  provides the highest probability of success.

### 4.1.3 Delay Analysis

We now evaluate the average transmission delay over an intermittently connected wireless link using the two retransmission schemes. Our approach is to first determine the probability that a packet transmission will be successful in a single active-inactive cycle of the source node. As illustrated in Fig. 4.6, the total transmission delay is equal to the period of time covering the expected number of active-inactive cycles required before the packet transmission is successful plus the expected delay involved within the active period where the packet is delivered.

The overall probability of success for transmitting a packet in a single active-inactive cycle depends on the probability of success at the very first transmission after waking up from sleep state, and that from retransmission, if the first transmission is not successful. In the following, we find the success probability of the first transmission, the maximum success probability in a single active-inactive period that is achievable using each retransmission policy, and the expected delay involved within an active period, to obtain the overall delay.

The success probability of the very first transmission attempt after waking up from a long sleep period depends on whether the receiver is active or not during that transmission. Hence, we find the active probability of the receiver at any random slot.

Let's consider that the receiver has enough energy to be in the active period for an average  $(\mu_a + 1)$  units of time. Within this time, if an average of  $\alpha$  overhearing occurs, we get  $\mu_a \cdot P_o = \alpha$  or,  $\mu_a = \frac{\alpha}{P_o}$ . Using a similar approach as (4.1), we may

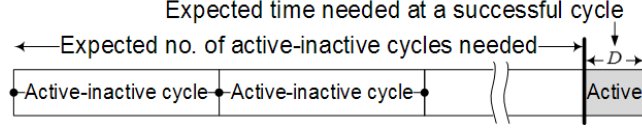


Figure 4.6: Calculation of the packet transmission delay.

write

$$\begin{aligned} \alpha E_o + (\mu_a - \alpha) E_a &= E_h - E_r & (4.11) \\ \text{or, } \alpha(E_o - E_a) + \mu_a E_a &= E_h - E_r \\ \text{or, } \mu_a \cdot P_o(E_o - E_a) + \mu_a E_a &= E_h - E_r \\ \text{or, } \mu_a &= \frac{E_h - E_r}{P_o(E_o - E_a) + E_a} \end{aligned}$$

Since the time between successive energy arrivals is geometrically distributed with parameter  $P_e$ , the average interval is  $\mu_e = \frac{1}{P_e}$ . When  $\mu_a$  is much smaller than  $\mu_e$  (as in the case of intermittently connected network), the probability that the destination is active at a random time slot is approximately  $\frac{(\mu_a + 1)}{\mu_e}$ . Hence, the probability of success at the very first transmission can be written as

$$P_1 \approx \left[ \frac{(\mu_a + 1)}{\mu_e} \right] P_c \quad (4.12)$$

Using (4.7), (4.10), and (4.12), we can write the overall success probability at any active-inactive cycle associated with predictive retransmission as

$$P_{SP} = P_1 P_c + (1 - P_1 P_c) P_m^p \quad (4.13)$$

If a transmission is successful in an active period, the expected time required for



the success from the beginning of that active period can be written as

$$E_p[D] = \frac{1}{P_{SP}}(P_1P_c + (1 - P_1P_c)P_m^p(T_o^p + 1)) \quad (4.14)$$

Similarly, the overall success probability associated with back to back retransmissions is

$$\begin{aligned} P_{SB} &= P_1P_c + (1 - P_1P_c)(P_eP_c) + \dots \\ &+ (1 - P_1P_c)(1 - P_eP_c)^{\beta-1}(P_eP_c) \\ &= P_1P_c + (1 - P_1P_c)P_m^b \end{aligned} \quad (4.15)$$

Consequently, the expected time required for a success from the beginning of an active period is

$$\begin{aligned} E_b[D] &= \frac{1}{P_{SB}}(P_1P_c + 2(P_eP_c)(1 - P_1P_c) + \dots \\ &+ (1 - P_1P_c)(1 - P_eP_c)^{\beta-1}(P_eP_c)(\beta + 1)) \\ &= \frac{1}{P_{SB}}(P_1P_c + \\ &\sum_{m=2}^{\beta+1} m(P_eP_c)(1 - P_eP_c)^{m-2}(1 - P_1P_c)) \end{aligned} \quad (4.16)$$

The length of an average active-inactive cycle is equivalent to the average energy arrival interval  $\mu_e$ . If we denote the overall success probability at any cycle in general by  $P_s$  and the expected delay at a successful cycle by  $\bar{D}$ , we can express the expected

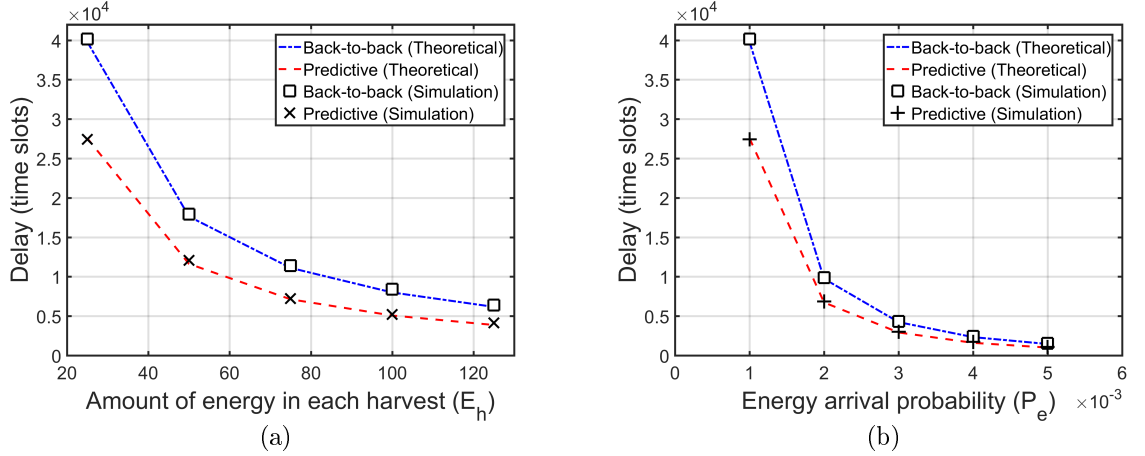


Figure 4.7: Delay performance in an intermittently connected wireless link using predictive and back-to-back retransmissions.

overall delay as

$$\begin{aligned}
 E[D] &= \bar{D}P_s + (\bar{D} + \mu_e)P_s(1 - P_s) \\
 &\quad + (\bar{D} + 2\mu_e)P_s(1 - P_s)^2 + \dots \\
 &= \bar{D}P_s + \bar{D}P_s(1 - P_s) + \bar{D}P_s(1 - P_s)^2 + \dots \\
 &\quad + \mu_e P_s(1 - P_s) + 2\mu_e P_s(1 - P_s)^2 + \dots \\
 &= \bar{D}P_s \sum_{i=0}^{\infty} (1 - P_s)^i + \mu_e(1 - P_s) \sum_{j=1}^{\infty} j P_s(1 - P_s)^{j-1} \\
 &= \bar{D}P_s \frac{1}{1 - (1 - P_s)} + \frac{\mu_e(1 - P_s)}{P_s} \\
 &= \bar{D} + \frac{\mu_e}{P_s} - \mu_e
 \end{aligned} \tag{4.17}$$

To validate these results, we perform simulations written in C++, which are based on a single source-destination pair. The source and destination nodes randomly harvest energy and consume that from ambient activities. At time slot 5000, the source generates a packet and inserts that into the transmission queue. We then record the time required to forward the packet to the destination. The simulation is repeated

10000 times and averaged for each observation. We also take into consideration that energy might be harvested while a node is still active. This additional energy is aggregated in an energy buffer. The size of the energy buffer is assumed to be equal to  $3E_h$ . Results provided in Fig. 4.7 show that up to 37% improvement can be achieved through the proposed predictive retransmission scheme.

## 4.2 Cross-layer design with predictive retransmission and transmission Diversity

We now discuss the adoption of the MAC layer predictive retransmission scheme with routing layer transmission diversity schemes (unicast routing with cooperative relaying and opportunistic routing) to further enhance the delay performance.

### 4.2.1 Cooperative Relaying with Predictive Retransmissions

We first describe how the predictive retransmission procedure can be applied to cooperative relaying and then analyze the delay. When a transmitter's first attempt becomes unsuccessful, it calculates its optimal waiting time  $T_o^p$  before the next retransmission according to its current energy. After each unsuccessful retransmission attempt, if the node is left with some energy it finds the next optimum retransmission interval based on its current parameters. This process continues until the transmitter runs out of energy. To facilitate cooperative relaying, if any neighboring node overhears a transmission, it captures the packet and determines the intended receiver. If the receiver is also within the transmission range of that node, it waits to see if the receiver acknowledges the transmission from the source. If it does not overhear the acknowledgment, then it assumes that the transmitter's attempt was unsuccessful, and it considers to cooperate in forwarding the packet. The cooperator sets up its own  $T_o^p$  according to its energy buffer to help forward the packet.

To analyze the delay performance of the retransmission scheme with cooperative relaying, let's consider a scenario where a source and  $\kappa$  other cooperators are trying to forward a packet to the receiver. At any given instance, the probability that any node

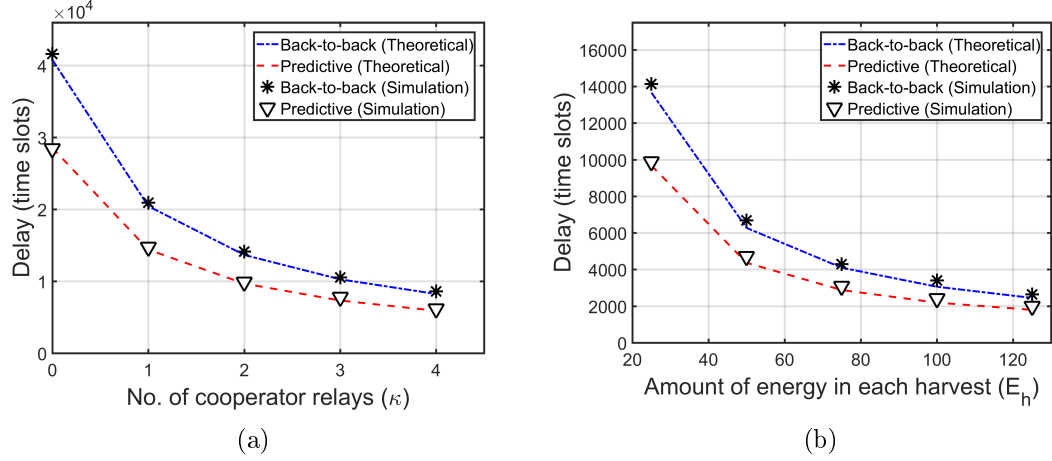


Figure 4.8: Delay performance in intermittently connected wireless link using cooperative relaying with different retransmission policies.

is trying to forward a packet is approximately,  $P_{\theta 1} \approx \frac{T_\theta}{\mu_e}$ , where  $T_\theta = (1 + T_o^p + 1)$ , for predictive retransmission, and  $T_\theta = (1 + \beta)$ , for back-to-back retransmissions. The probability that at least one among  $(\kappa + 1)$  nodes attempts to transmit the packet to the receiver can be expressed as

$$P_{\theta 1} = 1 - (1 - P_{\theta 1})^{\kappa+1} \quad (4.18)$$

For a single node, the success probability at any random time slot is,  $P_{s1} = \frac{P_s}{T_\theta}$ . Therefore, the overall probability of forwarding the packet with the help of  $(\kappa + 1)$  nodes at each slot is  $P_{s1}P_{\theta 1}$ . Hence, expected delay to successfully deliver the packet is

$$E[Delay_{(\kappa+1)}] \approx \frac{1}{P_{s1}P_{\theta 1}} \quad (4.19)$$

Numerical results obtained using the above model on the delay performance of cooperative routing over a wireless link with different number of relays are plotted in Fig. 4.8. The results indicate that substantial performance improvement (approximately 30%) can be achieved through the predictive retransmission policy over back-to-back retransmissions when cooperative relays are involved. Simulation results

validate these results as well.

#### 4.2.2 Opportunistic Routing with Predictive Retransmissions

Unlike unicast routing with cooperative relaying, opportunistic routing does not have a fixed (predefined) route. We propose that each transmission is forwarded by one or more nodes from a set of neighbors in the direction of the destination. Therefore, the predictive retransmission scheme in this case must be designed in such a way that at least one among the forwarder node set can be reached. If the number of nodes in such a forwarder set is  $\xi$ , then the success probability would be,

$$P_{OP} = P_w^t(T_w) \left[ 1 - \left( 1 - \sum_{x=1}^{T_w+1} [P_e(1 - P_e)^{(x-1)} P_w^r(T_w + 1 - x)] P_c \right)^\xi \right] \quad (4.20)$$

Therefore, once the first transmission in opportunistic routing fails, the transmitter estimates the retransmission interval according to the above equation and retransmits accordingly. Whenever a potential forwarder receives a data packet, it sends an acknowledgment to the source declaring its proposition as forwarder. Since multiple nodes might receive the data packet and send acknowledgments simultaneously, they use a contention window to randomly access the channel. After receiving acknowledgments from multiple potential forwarders, the source decides who will be the next forwarder and sends a confirmation to that node to make sure that only one copy of the packet gets forwarded.

### 4.3 Simulation Results

We evaluate the performance of the proposed predictive retransmission scheme with cooperative relaying and opportunistic routing using the *Castalia* simulator [94], which is an event-driven wireless sensor network simulator based on the *OMNeT++* platform. The energy consumption profile of a sensor node is obtained from the standard MICAz mote specifications. Table 4.3 summarizes some of these parameters. We mainly use end-to-end latency and packet loss as performance metrics for these

simulations. For a baseline comparison, we also obtain the performance using a traditional least cost (Dijkstra’s shortest path) routing protocol with back-to-back retransmissions. In all our simulations, 95% confidence interval fall within the 3% of the presented result.

We considered four different scenarios to evaluate the performance. These are,

- Event monitoring, single packet stream: Here a single node generates a packet to emulate the event reporting application. This packet is then forwarded to sink through multi-hop intermittently connected links. Nodes are arranged in a grid, and all nodes besides the source participate in forwarding packet from the same source.
- Event monitoring, overlapping packet stream: In this setup, we consider two neighbor nodes as event sources whose routing path to the sink overlap while forwarding the packet. This overlapping streams scenario is used to capture the effect of correlated data traffic
- Event monitoring, random node topology: Here, nodes are randomly placed in a square region and a random node is selected as the event source. This node then forwards the packet to the sink located at the center. This reflects more realistic sensor node deployment scenario.
- Data collection: In this case, a random subset of nodes within a grid is chosen as data sources that periodically generate packets and send to the sink. This setup demonstrates the typical data collection application scenario.

Details of these scenarios are described in the following.

#### 4.3.1 Event Monitoring: Single Packet Stream

In this configuration, 18 energy harvesting sensor nodes are placed in a uniform grid as illustrated in Fig. 4.9 (a). The node separation is assumed to be  $10m$  and the

Table 4.3: Simulation Parameters

Power consumed during transmission	42.55 mW
Power consumed during reception	73.54 mW
Power consumed during sleep	0.105 mW
Overall size of the transmission packet	130 B
Data transmission rate	250 Kbps
Sleep interval	125 ms
Listen interval	5 ms
Amount of energy in each harvest	52 mJ
Energy arrival probability	0.003

transmission radius is set to  $15m$ . At a certain time, node 7 generates a packet and tries to forward it to the sink. This represents an event detection scenario for node 7. We monitor the end-to-end latency in forwarding the packet with both cooperative relaying and opportunistic routing using predictive retransmissions. It must be noted here that each node may have different sets of forwarder nodes (opportunistic routing) or cooperator nodes (cooperative relaying) based on the chosen routing protocol. For example, in unicast routing with cooperative relaying, node 7 chooses 8 as the next hop which allows nodes 1, 2, 12 and 13 to have the opportunity to become cooperators for 7. When opportunistic routing is used, nodes 2, 8, and 13 can be in the forwarder set. We repeated the simulation for 100 times and took the average. The results are presented in Fig. 4.9 (b) and (c).

It can be seen that for both cooperative and opportunistic approaches, application of the predictive retransmission scheme provide significant improvements over back-to-back repetitive retransmissions. The average delay for all of the proposed schemes are lower than that obtained using shortest path routing, with as much as 62% delay reduction using opportunistic routing with predictive retransmissions. Also note that the primary route used in the cooperative scheme is the same as the shortest path route. This clearly illustrates the benefits of using cooperative transmissions, i.e.

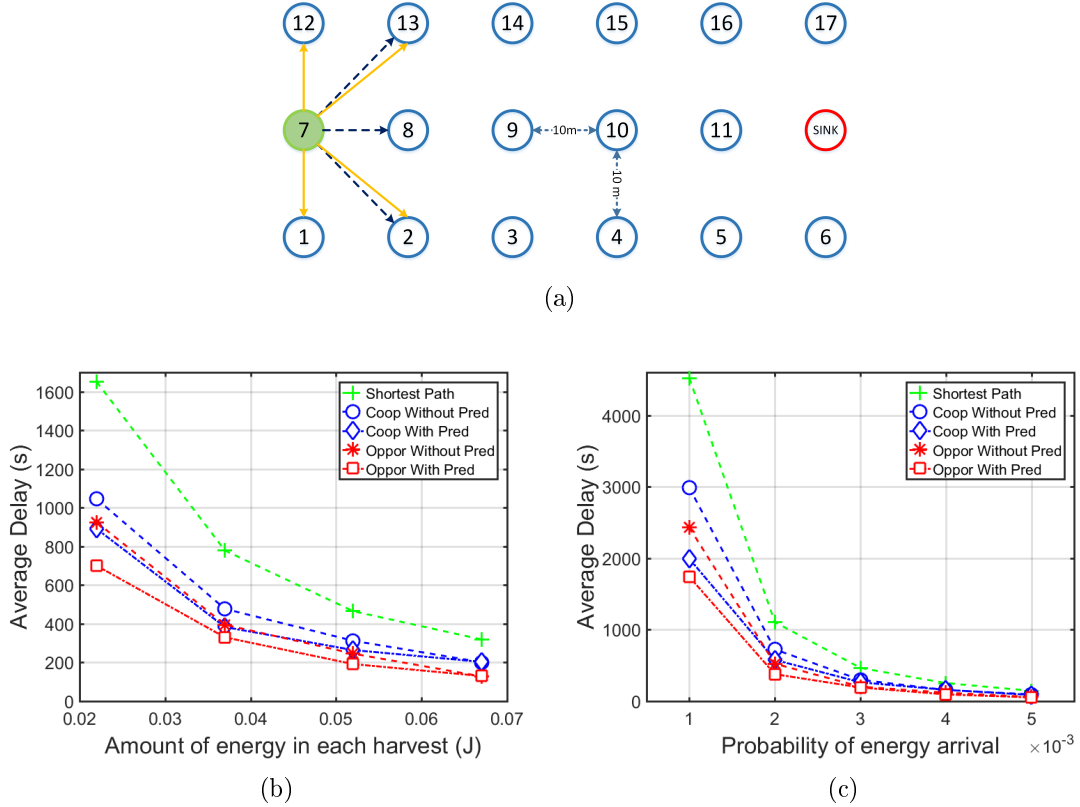


Figure 4.9: Delay performance for single packet stream in event monitoring application. Here, a) node configuration for the simulation, b) end-to-end delay at various harvested energy amounts, and c) end-to-end delay at various energy arrival probability

transmission diversity, and the predictive retransmission scheme in reducing the end-to-end delay in the ICSN.

### 4.3.2 Event Monitoring: Overlapping Packet Stream

In this case, we consider a network of 25 nodes that are arranged in a uniform grid as shown in Fig. 4.10 (a). At a certain time, we assume that nodes 7 and 13 simultaneously generate packets to be transmitted to the sink. This represents the scenario where multiple nodes detect the same event and try to report it to the sink. The multi-hop routes of both cases are chosen using a shortest-path algorithm and might have overlaps. We record the average of the end-to-end transmission delays from both paths obtained from a number of simulation runs and plot the averages in



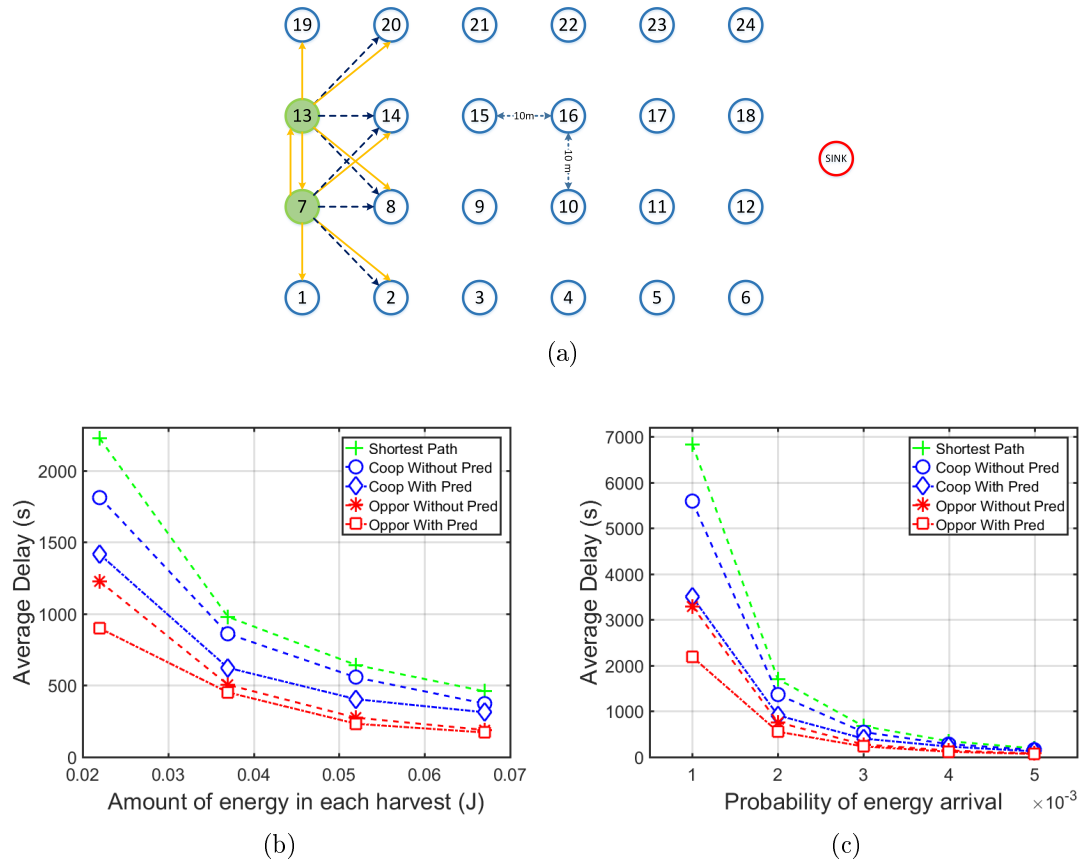


Figure 4.10: Delay performance for multiple stream in event monitoring application. Here, a) node configuration for the simulation, b) end-to-end delay at various harvested energy amounts, and c) end-to-end delay at various energy arrival probability

Fig. 4.10 (b) and (c).

It is evident from Fig. 4.10 that shortest path routing has the highest delay. In Fig. 4.10 (c) opportunistic routing with predictive retransmissions provides a significant 68% performance gain. However, we also notice that the performance improvement using the cooperative approach is low when predictive retransmission is not applied. This is mostly due to the excessive overhearing from nearby nodes (as two routing paths might share the same set of cooperating nodes). Furthermore, no attempt has been made to eliminate unnecessary cooperation attempts (for instance, cooperators may continue to relay even after the packet is already delivered by other cooperators). In our previous work [95] details of reducing these wasteful transmissions are

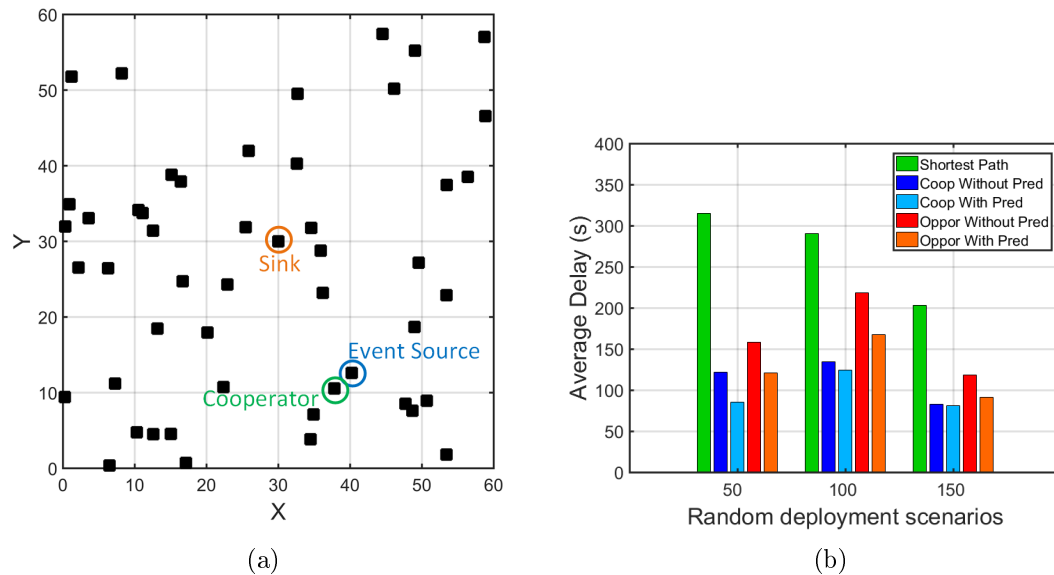


Figure 4.11: Delay performance for event monitoring application with random topology. Here, a) node configuration for the simulation, and b) end-to-end delay performance.

described.

### 4.3.3 Event Monitoring: Random Node Topology

In this scenario, nodes are randomly distributed over a  $60 \times 60$  meter square region using a uniform (random) distribution, as illustrated in Fig. 4.11 (a). The sink is located at the center. We consider three different node densities with 50, 100 and 150 nodes deployed over the region. For all the simulations, we chose a single source node placed at a random location. We then record the end-to-end latency in forwarding a packet from the source to the sink with various schemes. Results obtained from simulations are presented in Fig. 4.11 (b), which show that significant improvements are achieved with the predictive retransmission scheme in these scenarios as well.

Here, one interesting observation is that sometimes cooperative relaying outperforms opportunistic routing. This is due to the fact that in opportunistic routing, most nodes do not have more than one node in the forwarder set that can provide

routing progress. In cooperative relaying, however, any node within range of the transmitter and the next-hop node can relay on behalf of the transmitter, even if it is not closer to the destination. An illustration is depicted in Fig. 4.11 (a), where the source gets the cooperation from a neighbor that is the same distance as that of the source from the destination, and would not have been involved in opportunistic routing. In this simulation setup, we achieved upto 73% gain compared to traditional shortest path routing.

#### 4.3.4 Data Collection

We now consider a data collection scenario, where a random subset of nodes are selected as sources that periodically transmit data packets to the sink. Here, we consider that the ICSN is deployed in a uniform grid as shown in Fig. 4.12 (a). We consider the data transmission interval to be sufficiently large so as to avoid buffer overflow and congestion problems, so that the packet loss (Fig. 4.12 (c)) is low for all cases. Results presented in Fig. 4.12 (b) show that significant improvement (upto 41%) is achieved with the proposed predictive retransmission scheme when applied to either opportunistic or cooperative routing, in comparison to shortest path routing.

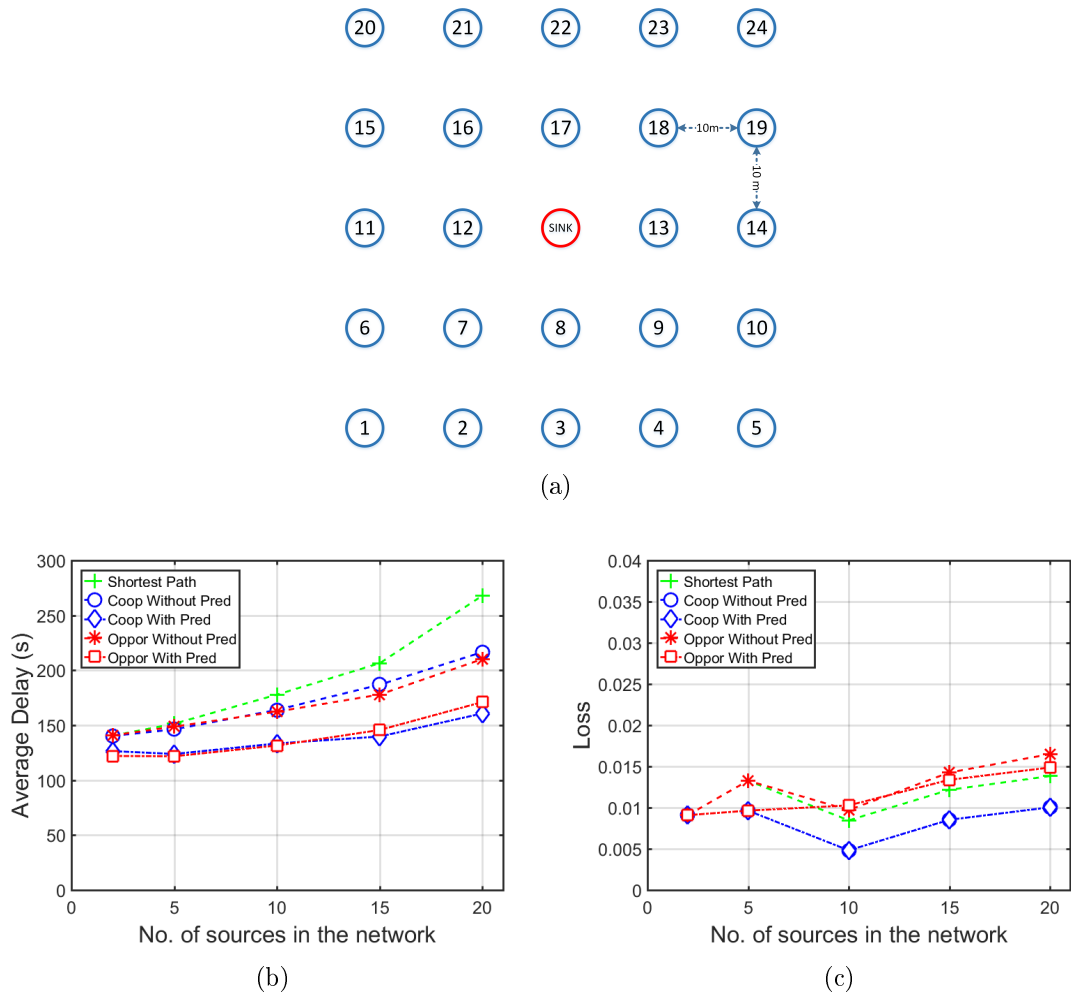


Figure 4.12: Delay performance for data collection application. Here, a) node configuration for the simulation, b) delay at various harvested energy amounts, and c) packet loss rate with finite buffer size.

## CHAPTER 5: DELAY MINIMIZATION IN RF ENERGY HARVESTING SENSOR NETWORKS

RF energy harvesting, though minuscule, can be a relatively predictable and stable source for energy supply [12, 69]. Often dedicated RF transmitters are placed at the sink to add to the small amount of energy harvestable from the ambient RF environment. With current and continuously evolving RF energy harvesting technology, this can be a sustainable source of energy for low power WSNs within short distances. However, due to the large attenuation in RF propagation, the proximity of the node to the RF transmitter highly dictates its harvest capabilities. Energy harvest rate falls exponentially as nodes move further away from the RF source. This inhomogeneous energy availability poses a unique challenge for delay minimization in such ICSN since nodes' energy demand does not necessarily match with their spatially correlated harvest rate. In this chapter, we first examine the energy harvest and delay characteristics of a typical RF energy harvesting WSN. We demonstrate the issue of inhomogeneous energy harvest and its impact on delay performance through simulations. Next, we explore the possibility of balancing the energy consumption with respect to the non-uniform energy availability by shifting the load of packet transmission process to the parent using a parent-triggered transmission scheme. Finally, we develop an optimal energy allocation strategy that helps the children's packet forwarding effort by effectively distributing the parent nodes' energy between transmission to the next hop and receiving from the child nodes.

## 5.1 Delay Characteristics and Motivation

In this section, we study the RF energy harvesting network characteristics and discuss the latency issues associated with it. To fully understand the RF energy harvesting network, let's first look at the typical amount of energy that can be harnessed in such networks. A popular commercially available hardware platform for RF energy harvesting in WSN is the *Powercast* [47,51,96,97] source and harvester. Their P2110-EVAL-01 development kit [98] comes with a 3 W, 915 MHz transmitter (TX91501) equipped with an integrated 8 dBi antenna. It also consists of a P2110 Powerharvester Receiver and an associated 6 dBi patch antenna. Plugging these parameters into the Friis transmission equation,

$$P_r = P_t + G_t + G_r + 20 \log_{10}\left(\frac{\lambda}{4\pi d}\right) \quad (5.1)$$

where  $P_r$ ,  $P_t$  represent the received and transmitted powers (in dBm);  $G_t$ ,  $G_r$  represent the transmitter antenna gain and receiver antenna gain (in dBi);  $\lambda$  is the wavelength; and  $d$  is the distance between the transmitter and the receiver. The corresponding variation of  $P_r$  with respect to  $d$  is illustrated in Fig. 5.1 (a). It can be observed that the received power falls exponentially, and it falls below 12 dBm (cut-off RF input power for the P2110 receiver) after only 28.5 meters from the RF source. Furthermore, Fig. 5.1 (b) provides a simple approximation of the high spatial dependency of harvesting rates in such networks.

Interestingly in multihop sensor networks, the traffic load at the sensor nodes also drops as the hop distance increases from the sink. To evaluate this, we simulated a RF energy harvesting ICSN in the *Castalia* simulator [94] using the energy consumption profile of the MICAz sensor node. Simulation parameters are summarized in Table 5.1. In this simulation, 25 nodes are arranged in a uniform grid and the sink is located at the center which also hosts an RF transmitter (see Fig. 5.2). Node separations

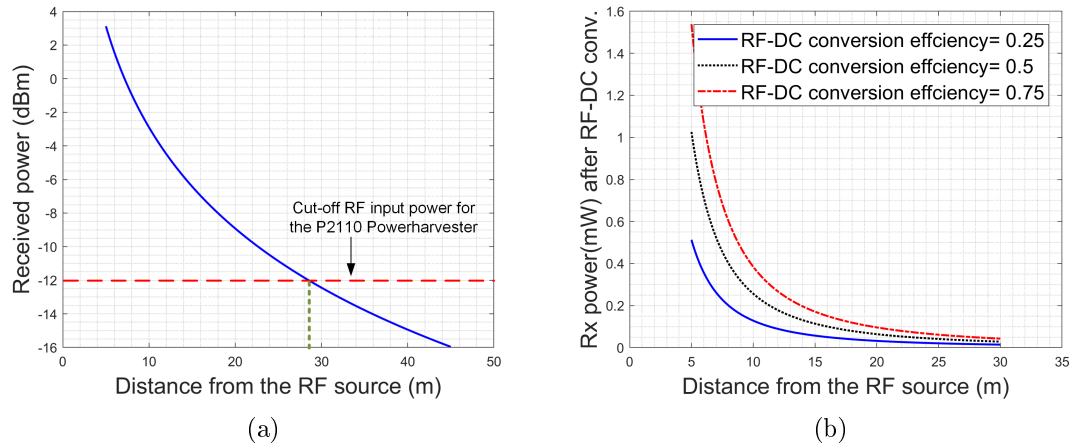


Figure 5.1: Received power and harvesting characteristics at different distances from the RF source.

are assumed to be  $10m$  and the transmission radius is set to  $15m$ . We assume that nodes are equipped with an out-of-band RF energy harvester where energy harvesting and data transmission take place in different frequency bands. Nodes become active by accumulating  $E_{th}$  amount of energy in its storage. After becoming active, a sender node transmits packets using the B-MAC [54] protocol where a long preamble is transmitted before the data transmission. The number of back-to-back retransmissions that can take place depends on the amount of energy harvested and the channel activity (each node performs carrier sensing before transmission). Other nodes after becoming active, listen to the channel using LPL. All nodes periodically generate packets at exponentially distributed random intervals that are large enough to avoid potential buffer delays. Packets are then forwarded to the sink using opportunistic routing. Here any node that receives a packet and can make a routing progress, sends an acknowledgment to the sender by randomly choosing a slot. The sender node then declares the node from whom it successfully received the first acknowledgment as its next forwarder.

Results presented in Fig. 5.3 (a) show that the traffic load of the nodes that are further away from the sink drops in a similar manner as their energy harvest rate (see

Table 5.1: Simulation Parameters

Power consumed during transmission	42.55 mW
Power consumed during reception	73.54 mW
Power consumed during sleep	0.105 mW
Power consumed during inactive mode	0 mW
Total energy consumed in one transmission	6.62 mJ
Energy harvest threshold $E_{th}$	20 mJ
Max transmission capacity in each active period	3
Overall size of the transmission packet	130 B
Data transmission rate	250 Kbps
Sleep interval	125 ms
Listen interval	5 ms

Fig. 5.3 (b)). This energy harvesting characteristic is rather desirable since it matches with the offered traffic load of the nodes. However, once we look at the end-to-end delay performance in Fig. 5.3 (c), we see that the nodes that are further away suffers from extremely large latency. Also, they have very high retransmission numbers (Fig. 5.3 (d)) which indicates that their energy consumption per packet is very high even though their harvest rate is low. Note that this high retransmission numbers mainly due to their extremely low duty cycle rate (as low as 0.003). This uneven energy consumption in forwarding a packet motivates us to come up with design strategies that will aid the nodes that are further away (at the expense of energy consumed by their parents that closer to the sink/RF source) and subsequently reduce the end-to-end latency. In the following sections, we explore two schemes to achieve this goal.

## 5.2 Parent vs Child Triggered Data Transmission

In the previous section, we demonstrated that in a two-hop network, child nodes have to put relatively more effort in forwarding a packet compared to its parent, even though they harvest exponentially less energy. In this section, we explore par-



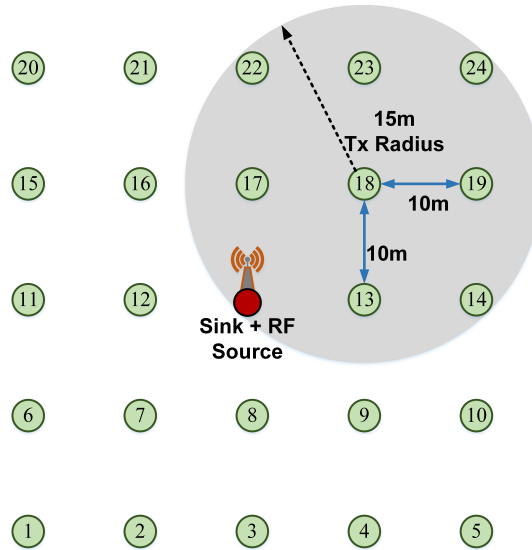


Figure 5.2: Node configuration for RF energy harvesting simulation.

ent vs child triggered data transmissions to offload some of the packet forwarding effort from the child to its parent. We consider the child triggered data transmission scheme as simply the B-MAC protocol we discussed in chapter 2. In contrast, the parent triggered transmission scheme (illustrated in Fig. 5.4 (a)) is the opposite of B-MAC where a potential parent always sends the preamble and a child periodically wakes up to listen to the channel for preamble activity from its parent. After detecting a preamble, it remains awake until the end of the preamble transmission and transmits a data packet immediately after that. An acknowledgment from the parent may complete the transmission process. Please note that this is also different from traditional receiver-initiated schemes [59] where receiver initiates the transmission by periodically transmitting small beacons and the child continuously listens to the channel. We recognize that since energy consumed in reception and transmission are almost similar [91], the action of a child sending a preamble in B-MAC compared to the child continuously listening to the channel in traditional receiver-initiated scheme by itself does not provide any benefit, i.e. does not take away much of the burden from the child. In case of parent-triggered transmission, however, the active duration

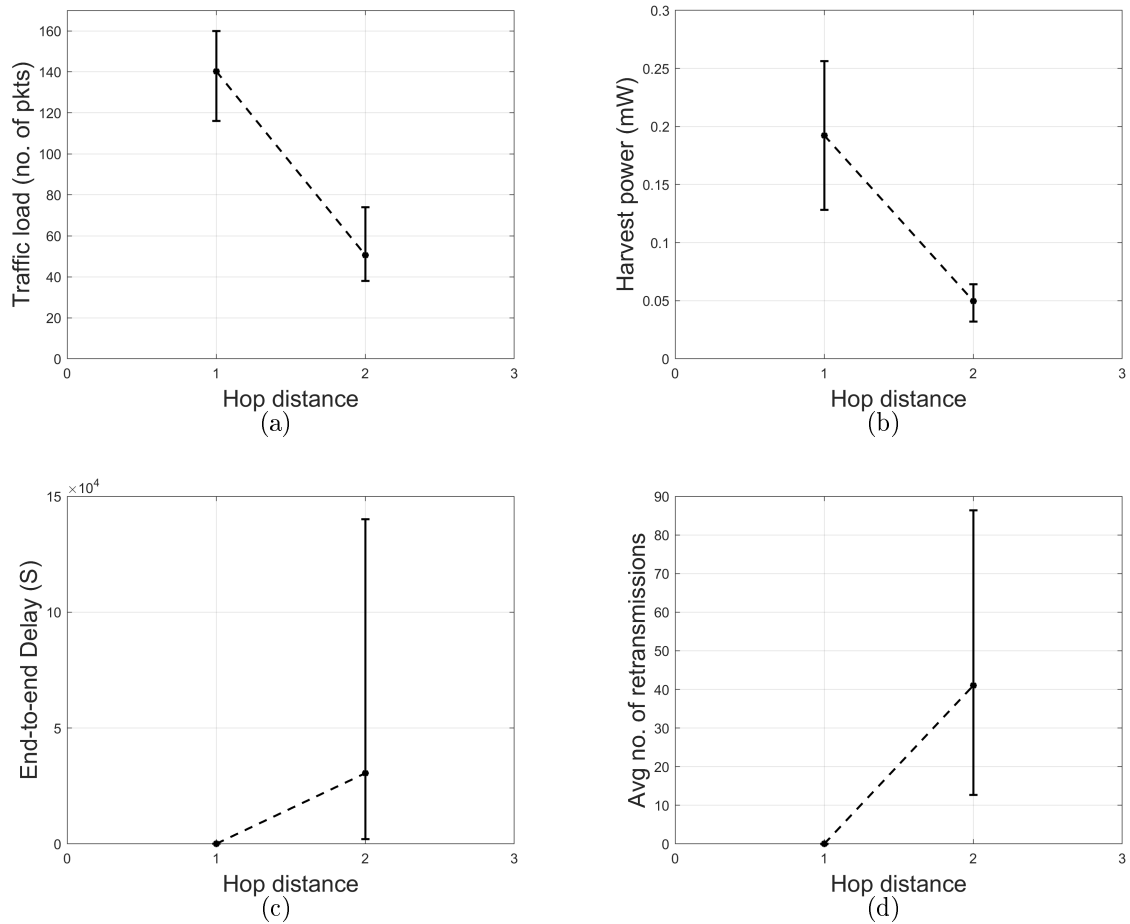


Figure 5.3: a) Traffic load b) received power c) end-to-end latency and d) average retransmissions per packet at different hop distances from the sink.

of the child increases significantly compared to the child-triggered (which is actually B-MAC) transmission, since it only has to spend a small amount of energy in each periodic listen activity. We claim that the benefits of having a child with a larger active duty cycle (ratio of active duration to cycle duration) by letting its parent trigger the transmission outweighs the benefit of having a parent with larger active duty cycle by letting child trigger the transmission. In the next section, we compare the two schemes by formulating the success probability associated with the parent vs child triggered transmission schemes.

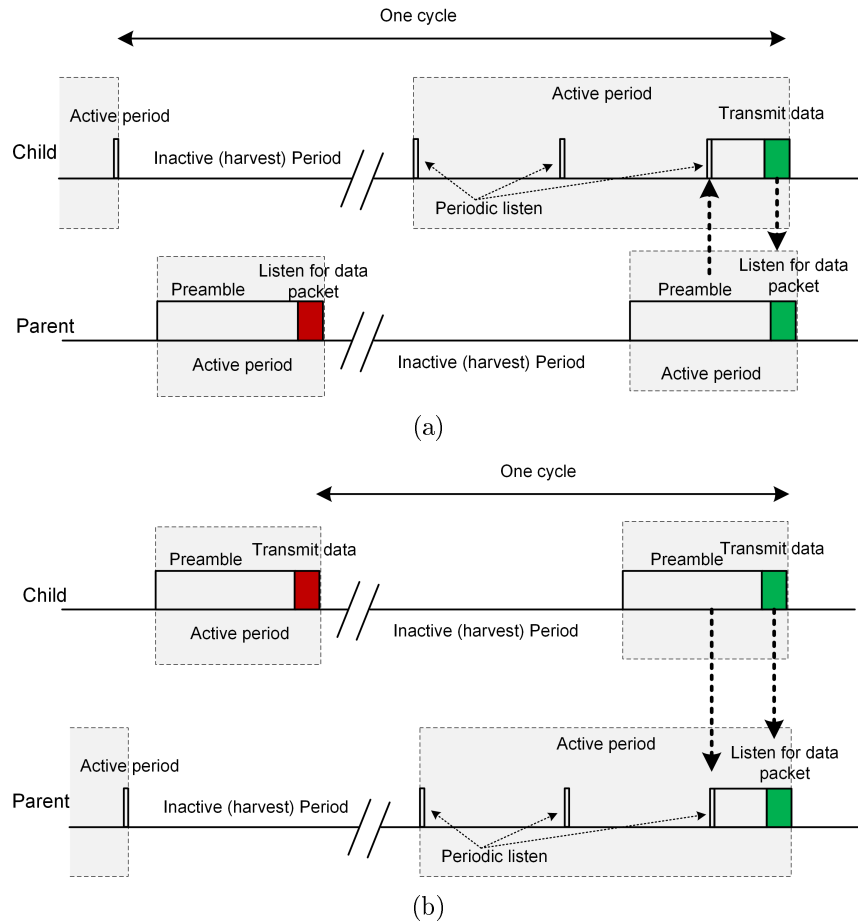


Figure 5.4: a) Parent triggered data transmission b) child triggered data transmission.

### 5.2.1 Success Probability of Parent vs Child Triggered Transmission

In the following, we formulate the success probability associated with the data transmission attempts of the child. We consider a simple two-node scenario where a child wants to forward a packet to its parent. We first consider that the time is slotted and nodes randomly wake up within each slot. We find the successful data forwarding probability from the probability of overlap between nodes active periods. Next, we consider that the child coarsely knows the active-inactive schedule of its parent by obtaining the information during each successful data transmission. Due to the randomness in radio propagation, the harvest rates are not constant, and nodes experience random variations in their schedules. This gives rise to an uncertainty in

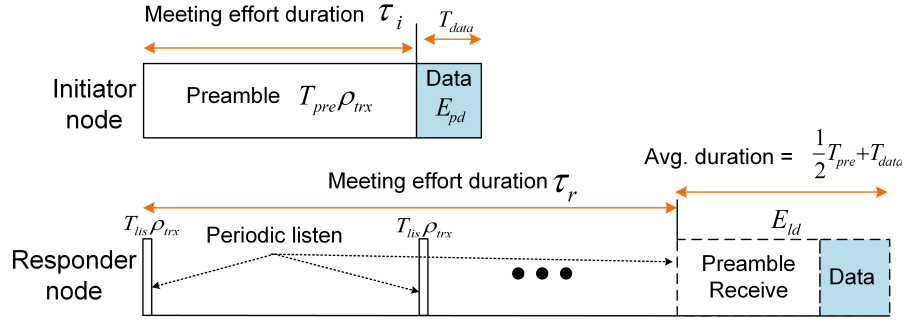


Figure 5.5: Energy consumption at various section of the active period.

the successful data transfer process even though the child tries to synchronize its data transmission with the parent's active period (learned from a past data exchange). We formulate the probability based on the overlapping probability of the child's attempt and parents active duration.

Let's consider that nodes wake up from their inactive harvest mode by accumulating  $E_{th}$  amount of energy in its storage. Power consumed in transmission and reception is similar and denoted by  $\rho_{trx}$ . The preamble length is  $T_{pre}$ , and it consumes  $T_{pre}\rho_{trx}$  amount of energy to transmit a preamble. This is illustrated in Fig. 5.5. When a node, either a child or a parent, takes the role of transmitting preambles (we call it an initiator node), it spends an additional  $E_{pd}$  amount of energy for transmitting a data packet or to receive a data packet after the preamble. Therefore, with a harvest threshold  $E_{th}$ , the preamble duration can be written as  $T_{pre} = (E_{th} - E_{pd})/\rho_{trx}$ . This is also the effective duration when an initiator node seeks a potential responder to establish a link. We name it the *meeting effort duration* of the initiator,  $\tau_i$ . If its harvest rate is  $H_i$ , then the length of the inactive period is  $E_{th}/H_i$ . Hence, the length of one active-inactive cycle of the initiator is,  $T'_i = \tau_i + T_{data} + (E_{th}/H_i)$  where  $T_{data}$  represents data transmission or reception duration. On the other hand, when a responding node periodically wakes up once in every preamble duration, and listens to the channel for  $T_{lis}$  amount of time, it will spend its overall harvested energy  $E_{th}$  into those small chunks of listen pulses. We can then represent responder's

*meeting effort duration* by,  $\tau_r = T_{pre} \cdot (E_{th} / (\rho_{tx} \cdot T_{lis}))$ . As the responder node detects a preamble, it may detect it anywhere within the length of preamble  $T_{pre}$ . Therefore, a responder nodes on an average captures half of the preamble before it can receive the data. We assume that responder node spends an average  $E_{ld}$  amount of energy for capturing a preamble and then transmit or receive data (see Fig. 5.5). This energy is harvested during the first harvest period after the packet arrival and buffered until actual packet reception. The duration of the responder node's first cycle is  $T_r = \tau_r + ((E_{th} + E_{ld}) / H_r)$ , due to additional  $E_{ld}$  harvest requirements, and subsequent period is  $T'_r = \tau_r + (E_{th} / H_r)$  provided that no successful transmissions take place. Considering that the time between successful packet transfer is large compared to the time required to harvest  $E_{ld}$  amount of energy, we ignore this to simplify our formulation. In the following, we formulate the success probabilities associated with both schemes.

#### 5.2.1.1 Random wake up without any prior information

Here we formulate the success probability when nodes randomly delay the start of their active period within a slot. The energy harvested during one slot is used to stay active during the next slot, therefore, the length of the meeting effort duration depends mainly on the slot duration. We assume that the maximum meeting effort duration length is fixed and independent of when the node started its active period in the prior slots. If we normalize the meeting effort duration by the slot time and denote it by  $D$ , and the start time from the beginning of a slot by  $t$  (see Fig. 5.6), then the event where two nodes meeting effort durations overlap can be written as,

$$P_{s1} = \{(t_i, t_r) | 0 \leq (t_r - t_i) \leq D_i \vee 0 \leq (t_i - t_r) \leq D_r, 0 \leq (t_r, t_i) \leq 1\} \quad (5.2)$$

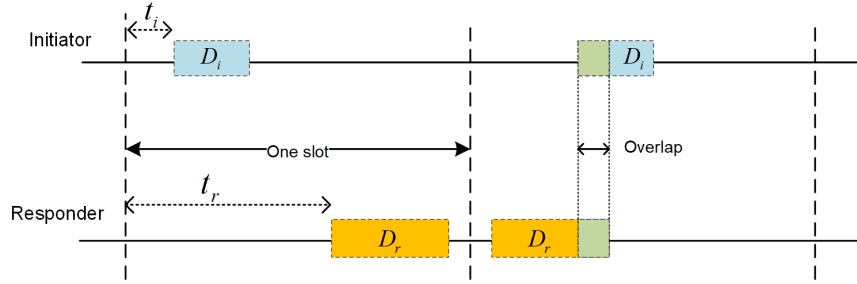


Figure 5.6: Scenario where nodes randomly wake up within a slot.

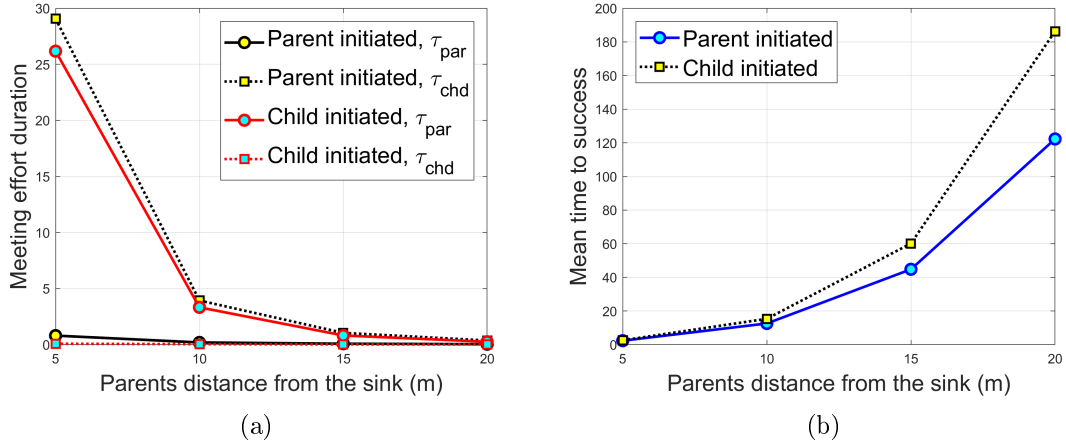


Figure 5.7: For child vs parent initiated transmissions a) variations in meeting effort durations b) mean time to overlap.

This is a classic meeting probability problem and can be written as [99],

$$P_{s1} = D_i + D_r - 0.5D_i^2 - 0.5D_r^2 \quad (5.3)$$

Using the parameters from P2110-EVAL-01 development kit, and considering a child-parent separation distance of 10m, we demonstrate in Fig. 5.7 (a) that parent initiated transmissions always provide longer meeting effort durations compared to child-initiated transmissions. This is because the benefit of having a small number of wakeups of the responder with longer intervals (since intervals depend on the initiator's preamble length) outweighs the benefit of a higher number of wakeups

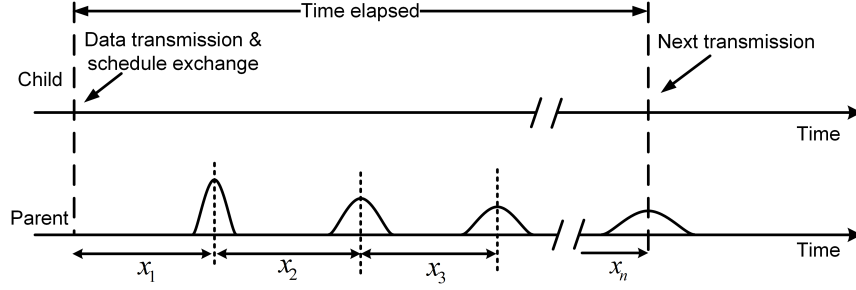


Figure 5.8: Success probability estimation.

with smaller intervals. This ultimately affects the average time needed to successfully deliver a packet which is illustrated in Fig. 5.7 (b).

#### 5.2.1.2 Waking up according to statistical information

In this section, we derive the probability of success when harvest rates are not constant and nodes exchange some scheduling information during each successful data transfer. Due to several factors such as multi-path propagation and shadow fading affecting the radio propagation, the harvest rates are not constant in reality. To account for these effects, we represent the initiator and responder durations by  $T_i = T'_i + X_{\sigma_i}$  and  $T_r = T'_r + X_{\sigma_r}$ , respectively. Here  $X_{\sigma}$  is a Gaussian random variable with zero mean and  $\sigma^2$  variance. When a child wants to forward a packet, it estimates how much time has elapsed since the last schedule exchange. Let's denote this by  $T_{elp}$ . It then calculates the next approximate wake up time of the parent by assuming that parent should have completed  $n = \lceil \frac{T_{elp}}{T_{par}} \rceil$  cycles in the mean time. Here,  $T_{par}$  is the scheduled cycle duration of the parent node, and it depends on whether the child or the parent initiates the transmission. We can represent the  $i$  th cycle duration as an independent normally distributed random variable  $x_i$  with  $T_{par}$  mean and  $\sigma_{par}^2$  variance, i.e.,  $x_i \sim \mathcal{N}(T_{par}, \sigma_{par}^2)$ . This is illustrated in Fig. 5.8. Therefore, the distribution of wake up time after  $n$  cycles can be represented as a sum of  $n$  normally

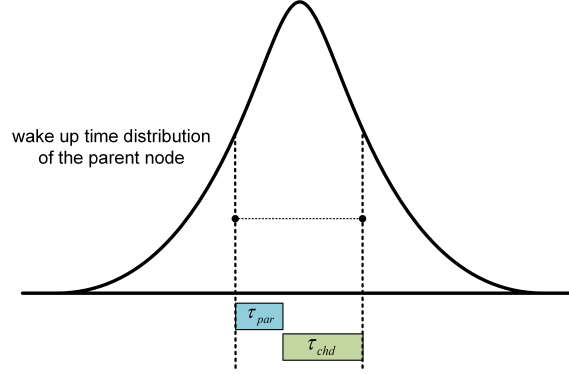


Figure 5.9: Maximizing the likelihood of a successful transmission.

distributed random variables,

$$\begin{aligned}
 X &\sim \sum_n x_i & (5.4) \\
 &\sim \mathcal{N}\left(\sum_n T_{par}, \sum_n \sigma_{par}^2\right) \\
 &\sim \mathcal{N}(nT_{par}, n\sigma_{par}^2)
 \end{aligned}$$

A key objective is to maximize the probability of successful transmission which is achieved if the child can transmit within the meeting effort duration of the parent, or the parent wakes up from the inactive mode within the child's meeting effort duration. Since  $X$  also has a normal distribution this can be achieved when the child transmits at  $[nT_{par} - 1/2(\tau_{par} + \tau_{chd}) + \tau_{chd}]$  so that their combined meeting effort spreads symmetrically from the center of the bell curve. This is illustrated in Fig. 5.9. The success probability can then be written as,

$$P_{s2} = P\left(nT_{par} - \frac{1}{2}(\tau_{par} + \tau_{chd}) \leq X \leq nT_p + \frac{1}{2}(\tau_{par} + \tau_{chd})\right) \quad (5.5)$$

When  $\tau_{par}$  and  $\tau_{chd}$  are fixed, the success probability depends on the standard deviation  $\sigma_{par}$ , which ultimately depends on the number of cycles that the parent has completed since the last schedule exchange and the deviation associated with



each cycle. If we consider the standard deviation is proportional to the period length due to several random phenomena such as RF propagation, clock drift, and variation in ambient consumption (sensing and processing), it can be shown that the parent initiated transmission performs better than the child initiated transmission.

**Proposition.** *When  $\sigma_{par} \propto T_{par}$ , parent initiated transmission performs better*

*Proof.* Let's consider the time elapsed since the last schedule exchange is  $T_{el}$ . Also consider that the parent's period length is  $T_{pi}$  when the parent initiates the transmission, and  $T_{ci}$  when the child initiates the transmission. Now the parent can complete  $\kappa_{pi} = T_{el}/T_{pi}$  cycles, or  $\kappa_{ci} = T_{el}/T_{ci}$  cycles based on the initiation strategy. For a fixed harvest threshold  $E_{th}$ ,  $T_{pi} < T_{ci}$ . Now if we consider,  $\sigma_{par} = w.T_{par}$ , then we can write the variances of  $X$  for both scenarios as,

$$\begin{aligned} \kappa_{pi}(wT_{pi})^2 &= \nu\kappa_{ci}(wT_{ci})^2 & (5.6) \\ \Rightarrow \frac{T_{el}}{T_{pi}}T_{pi}^2 &= \nu\frac{T_{el}}{T_{ci}}T_{ci}^2 \\ \Rightarrow \nu &= \frac{T_{pi}}{T_{ci}} \\ \Rightarrow \nu &< 1 \end{aligned}$$

Therefore, the variance of  $X$  is smaller when the parent initiates the transmission. This makes the success probability of parent triggered transmission higher.  $\square$

We present numerical results in Fig. 5.10 using the parameters from P2110-EVAL-01 development kit discussed earlier in this chapter. In Fig 5.10 (a), we kept the distance of parent and child constant at  $7m$  and  $15m$  respectively. We varied the time elapse since last schedule exchange and plotted associated probability. In Fig 5.10 (b), we consider the elapsed time as one cycle duration of child which represents the success probability of immediate transmission after a successful data transfer. We increase the distance of the parent from the sink while keeping the parent child distance constant

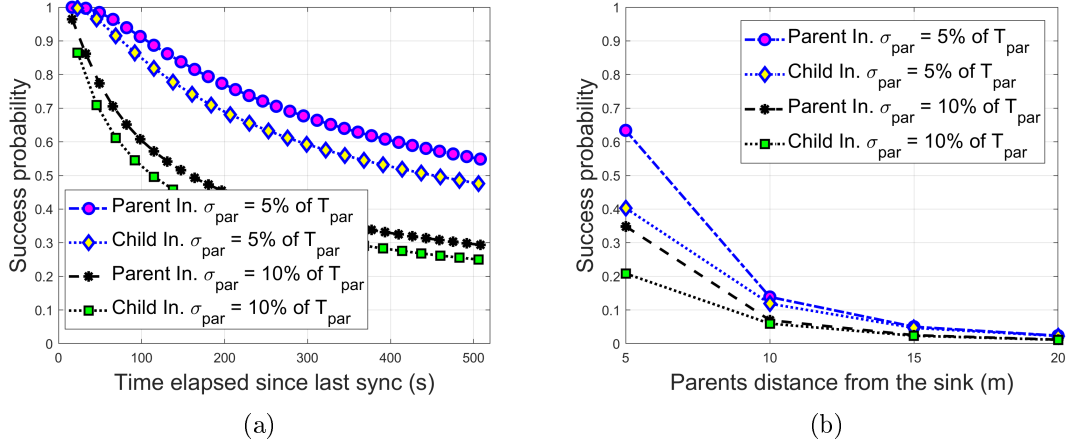


Figure 5.10: Probability of success with a) variable time elapsed since last schedule exchange b) different parent distances from sink.

at  $10m$ . Results show that parent initiated transmission can perform notably better than the child initiated transmission. In the next section, we further improve parent's assistance in child's forwarding process by allocating more parent's energy for data reception from the child.

### 5.3 Optimal Energy Allocation Between the Transmission and Reception Activities

Since parent nodes have higher harvest rate but consume less energy in forwarding a packet, they usually have surplus harvested energy that can be utilized to assist children's packet forwarding effort by allocating more energy for packet reception from the children. From our simulation study in section 5.1, we have seen that the child-parent link (two hops from the sink) experiences comparatively higher latency compared to the parent-sink link. Therefore the child-parent link causes a throughput bottleneck in the network. If parents optimally distribute their energy between the parent-sink link transmission and the child-parent link reception so that the maximum sustainable throughput can be achieved, it will reduce the overall end-to-end latency by reducing the long queuing delay of the child. In this section, we develop an optimal

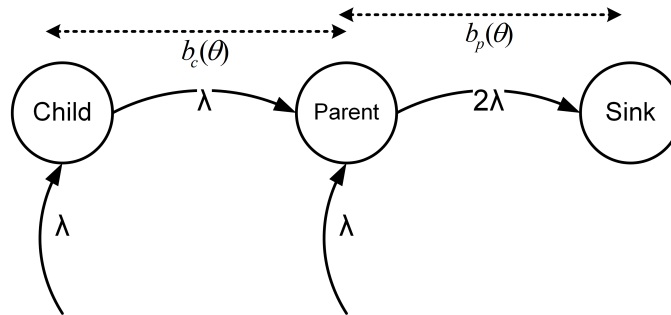


Figure 5.11: Optimizing throughput by effectively distributing parents energy.

energy allocation policy for the parent that achieves this maximum throughput while at the same time reducing queuing delay.

### 5.3.1 Optimal Policy

In the following we formulate an optimization problem so that parent's energy is optimally allocated between transmission and reception activities. We consider a two-node scenario illustrated in Fig. 5.11, where each node samples its environment and generates data packets at  $\lambda$  bits per second. The child node spends all of its energy for forwarding its own traffic while parent consumes a fraction of its harvested energy  $\theta.H_{par}$  to forward its overall traffic and  $(1 - \theta)H_{par}$  to receive packet from its child. Since the child spends all of its energy for transmission only, the maximum bit rate of the child-parent link,  $b_c$  and the parent-sink link,  $b_p$  is a function of  $\theta$ . We want to optimize the value of  $\theta$  such that the link rate (or packet service rate of a node) remains smaller than its traffic generation rate (or packet arrival rate), and at the same time the overall throughput  $\lambda$  is maximized. We can pose the problem as follows,

$$\begin{aligned}
& \text{maximize} && \lambda \\
& \text{subject to} && \lambda < b_c(\theta) && \text{(to stabilize child's packet queue)} \\
& && 2\lambda < b_p(\theta) && \text{(to stabilize parent's packet queue)} \\
& && 0 \leq \lambda \leq b_t, 0 \leq \theta \leq 1
\end{aligned}$$

In the following section, we first find the link rates as a function of  $\theta$  to solve this problem.

### 5.3.2 Data Rate of the Child-parent and the Parent-sink Links

Here, we formulate the maximum bit rate in the child-parent and the parent-sink link for a certain amount energy spent by the parent. In order to find this, we first find the expected delay in forwarding a packet in child-parent link, and then calculate the bit rate of both links from there.

Let's find the success probability associated with  $j$ th transmission attempt of the child. Consider  $\tau = \tau_i + \tau_r$ ,  $\sigma'_{chd} = \sqrt{j \cdot \sigma_{chd}^2}$ , and  $n'_j = \lceil \frac{T_{el} + (j-1)T_{chd}}{T_{par}} \rceil$ . Then the number of cycles parent can complete right after child's  $j$ th cycle such that child still has the opportunity to maximize its successful transmission attempt can be written as,

$$n_j = \begin{cases} n'_j, & \text{when } (j-1)T_{chd} + T_{el} \leq (n'_j T_{par} - 0.5\tau - \sigma'_{chd}) \\ n'_j + 1, & \text{otherwise} \end{cases} \quad (5.7)$$

The success probability associated with  $j$ th attempt  $P_{sj}$  can be found from equation 5.5 by substituting  $(1-\theta)H_{par}$  as parent's harvest rate. When a child has a saturated packet buffer, it will attempt a transmission at every cycle, therefore,  $T_{el} = T_{chd}$ . We assume that a packet is transmitted  $m$  number of times before it is dropped from the buffer. After that a node simply waits for the next global synchronization event. We consider that the mean time between the global synchronization event is  $\mu_{snc}$  where

$\mu_{snc} \gg T_{chd}$ . With this, we can formulate the expected delay in forwarding a packet which is the combination of expected delay if a packet transmission is successful within  $m$  attempts plus the expected delay if it can't become successful within that. This can be written as,

$$E[d_{pkt}] = \sum_{j=1}^m P_{sj} \left[ \prod_{k=1}^{j-1} (1 - P_{sk}) \right] \cdot j [\max(T_{chd}, T_{par})] \quad (5.8)$$

$$+ \left[ \prod_{j=1}^m (1 - P_{sj}) \right] \cdot \mu_{snc}$$

Let's assume that the data packet length is  $L$ , and the maximum bit rate of link based on the transmission power, modulation and coding scheme is  $b_t$ . Then the average bit rate of the child-parent link can be approximated as

$$b_c(\theta) = \frac{L}{E[d_{pkt}]} \quad (5.9)$$

assuming that the parent initiates the transmission. In the parent-sink link, the sink is always active, therefore, the bit rate of this link,

$$b_p(\theta) = \frac{L}{\frac{E_{pkt}}{\theta H_{par}} + 0.5T_{pre} + \frac{L}{b_t}} \quad (5.10)$$

where  $E_{pkt} = (0.5T_{pre} + \frac{L}{b_t})P_{trx}$  is the average energy required to capture a preamble and then transmit a data packet. In Fig. 5.12, we illustrated the variation of bit rates in both the parent-sink and the child-parent link for different fractional energy spent by the parent in transmission process. We see that regardless of the fraction, the link rates fall drastically as the nodes move away from the sink. Also, a much higher bit rate can be achieved for the parent-sink link compared to the child-parent link when the same amount of energy spent on both links. Therefore, the parent should spend most of its energy for the child-parent link. However, the parent also has to forward

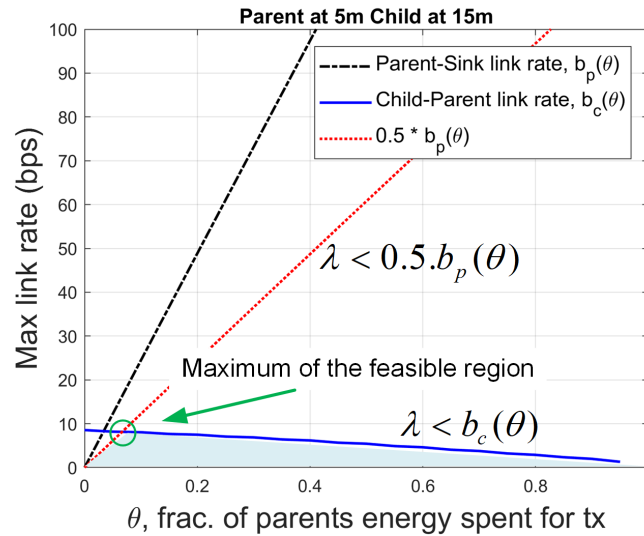


Figure 5.12: Bit rate of the child-parent and parent-sink link for different fractions of the parent's energy spend in transmission.

child's traffic, which requires that the parent-sink link should carry at least twice as much traffic as the child-sink link. Our goal is to find the optimal fraction of energy parent should spend such that the bit rates of both links are maximized.

This is a non-linear optimization problem. We used Matlab for solving this numerically and the corresponding performance results are illustrated in Fig. 5.13. In the left column, we present the fraction of harvested energy that a parent should spend for transmission to achieve the maximum supported bit rate. In the right column, we present  $\lambda$ , the maximum sustainable bit rate associated with that. Throughout this numerical evaluations, the default parent-child separation is kept  $10m$ , and the standard deviation is kept at 10%. We see that as the distance of the parent from the sink increases, it is required to spend more energy for itself since harvest rate falls exponentially making its forwarding harder. An interesting case is Fig. 5.13 (c), where the initial proximity of child ( $5m$  separation) to the sink urges parent node to spend relatively more energy for the reception to support a higher data rate of the child. We observe that the sustained throughput falls exponentially as nodes move further away due to lower harvest rate which is expected.

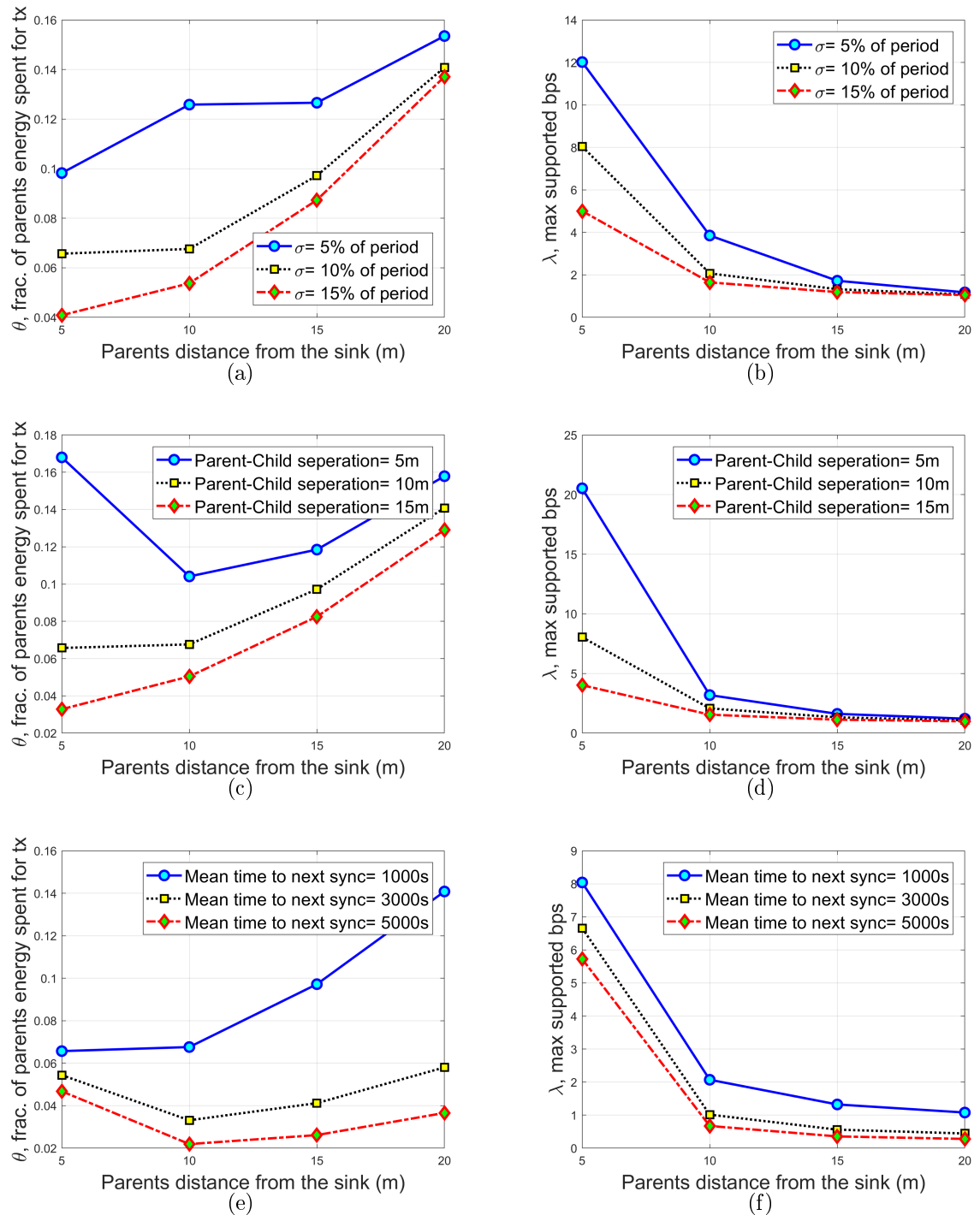


Figure 5.13: Maximum achievable throughput and the fraction of energy should be spent to sustain that.

## CHAPTER 6: CONCLUSIONS

In this research, we addressed the issue of minimizing the end-to-end transmission delay in energy harvesting intermittently connected sensor networks (ICSNs) characterized by random and asynchronous node outages. We assume that the nodes are powered by low-powered environmental harvesting units that have insufficient energy for maintaining continuous node operations, leading to the random outages. In such networks, it is important to optimally use the limited energy resources distributed among the harvesting nodes and utilize the unpredictable energy harvest in a timely manner to maximize the success probability of transmissions. We investigated three design approaches to address the issues.

First, we considered the neighbor cooperation for forwarding packets over a predefined unicast route. We developed a discrete-time Markov Chain model to analyze the link delay characteristics and quantified the benefits of cooperative relaying over unicast routes. Specific considerations were presented for minimizing the wastage of scarce energy resources while utilizing the benefits of cooperative relays. A two-hop cooperative relaying scheme Ephemeral Two-hop Opportunistic Cooperation (ETOC) is proposed that incorporated these considerations for minimizing the end-to-end transmission delay in a practical network setup. Results from multi-agent based computer simulations for ETOC were presented that show that up to 31.81% delay improvement can be achieved. Moreover, the benefits of ETOC were found to be high at the low levels of the energy harvesting, i.e. when the rate of link disconnection or intermittency is high.

Second, we developed an optimized retransmission scheme that determines the most suitable time to transmit based on the statistical characteristics of energy avail-



ability and usage at the nodes. Nodes have similar energy harvesting characteristics as mentioned above. However, they try to predict retransmission times after each unsuccessful packet transmission that can maximize the probability of successful packet delivery. The predicted retransmission interval is based on the node's current energy level and the characteristics of energy availability. We further incorporated this strategy into cooperative relaying over unicast routes and opportunistic routing to achieve transmission diversity. Performance evaluations obtained from computer simulations demonstrate that the proposed schemes can provide as much as 73% improvement on the end-to-end transmission delay in comparison to a traditional least-cost routing approach that uses back-to-back transmissions. The proposed predictive retransmission concept contributes to over 37% reduction in the transmission delay for unicast routing with cooperative retransmissions and up to 33% reduction in the case of opportunistic routing.

The work mentioned above addressed ICSNs where all nodes are assumed to have independent and identically distributed outage characteristics. In Chapter 5, we consider the case of RF energy harvesting ICSNs where harvesting is highly correlated to nodes' locations. To address the difference between the energy harvested by nodes closer to the energy source (e.g. sink), we explored parent vs child initiated transmissions and found that some of the packet forwarding efforts of the child can be offloaded to the parent by considering the parent initiated data transmission scheme. Our findings were obtained from different mathematical models and numerical results. We further facilitated offloading by developing optimization models that judiciously allocated the parent's energy into transmission and reception activities such that a higher overall networkwide throughput can be achieved.

In the future, our plan is to progress the offloading of packet forwarding efforts in RF energy harvesting networks. We believe that the RF energy harvesting has the potential to shape not only the future of WSNs but also wearable devices and inter-

net of things. One approach we are currently considering is to develop uncorrelated parent-initiated transmissions from a set of multiple potential forwarders. In a dense network, this might have an adverse effect due to the increased overhearing or might be challenging when intermittency in connectivity decreases. However, it would be an interesting study to find the tradeoffs between excessive energy consumption and latency minimization through theoretical analysis and simulations. We are also considering developing a distributed routing protocol with on-demand RF energy supply from a sink hosted RF transmitter with narrow beamforming.

The Performance evaluations obtained from the theoretical formulations, numerical results, as well as simulations, demonstrate the benefits of the proposed schemes. Our belief is that the design considerations studied in this research will provide a valuable insight into the future maintenance-free sensor network development.

## REFERENCES

- [1] G. Anastasi, M. Conti, M. Di Francesco, and A. Passarella, “Energy conservation in wireless sensor networks: A survey,” *Ad hoc networks*, vol. 7, no. 3, pp. 537–568, 2009.
- [2] T. Rault, A. Bouabdallah, and Y. Challal, “Energy efficiency in wireless sensor networks: A top-down survey,” *Computer Networks*, vol. 67, pp. 104–122, 2014.
- [3] M. Minami, T. Morito, H. Morikawa, and T. Aoyama, “Solar biscuit: A battery-less wireless sensor network system for environmental monitoring applications,” in *The 2nd international workshop on networked sensing systems*, 2005.
- [4] X. Jiang, J. Polastre, and D. Culler, “Perpetual environmentally powered sensor networks,” in *IPSN 2005. Fourth International Symposium on Information Processing in Sensor Networks, 2005.*, pp. 463–468, IEEE, 2005.
- [5] J.-M. Dilhac and M. Baffeur, “Energy harvesting in aeronautics for battery-free wireless sensor networks,” *IEEE Aerospace and Electronic Systems Magazine*, vol. 29, no. 8, pp. 18–22, 2014.
- [6] F. K. Shaikh and S. Zeadally, “Energy harvesting in wireless sensor networks: A comprehensive review,” *Renewable and Sustainable Energy Reviews*, vol. 55, pp. 1041–1054, 2016.
- [7] S. Sudevalayam and P. Kulkarni, “Energy harvesting sensor nodes: Survey and implications,” *IEEE Communications Surveys and Tutorials*, vol. 13, no. 3, pp. 443–461, 2011.
- [8] N. A. Bhatti, M. H. Alizai, A. A. Syed, and M. Luca, “Energy harvesting and wireless transfer in sensor network applications: Concepts and experiences,” *ACM Transactions on Embedded Computing Systems*.
- [9] M. Peigney and D. Siegert, “Piezoelectric energy harvesting from traffic-induced bridge vibrations,” *Smart Materials and Structures*, no. 22(9):095019, 2013.
- [10] Y. Li and R. Bartos, “A survey of protocols for intermittently connected delay-tolerant wireless sensor networks,” *Journal of Network and Computer Applications*, vol. 41, pp. 411–423, 2014.
- [11] N. Nakashima, H. Nishimoto, Y. Kawahara, and T. Asami, “Human detection system based on sensing through harvesting concept,” in *Internet of Things 2010 Conference*, 2010.
- [12] H. Nishimoto, Y. Kawahara, and T. Asami, “Prototype implementation of ambient rf energy harvesting wireless sensor networks,” in *IEEE Sensors*, pp. 1282–1287, IEEE, 2010.

- [13] D. Mishra, S. De, S. Jana, S. Basagni, K. Chowdhury, and W. Heinzelman, "Smart rf energy harvesting communications: Challenges and opportunities," *IEEE Communications Magazine*, vol. 53, no. 4, pp. 70–78, 2015.
- [14] X. Lu, P. Wang, D. Niyato, D. I. Kim, and Z. Han, "Wireless networks with rf energy harvesting: A contemporary survey," *IEEE Communications Surveys & Tutorials*, vol. 17, no. 2, pp. 757–789, 2015.
- [15] A. Nasipuri, R. Cox, J. Conrad, L. Van der Zel, B. Rodriguez, and R. McKosky, "Design considerations for a large-scale wireless sensor network for substation monitoring," in *IEEE 35th Conference on Local Computer Networks (LCN)*, pp. 866–873, IEEE, 2010.
- [16] I. Demirkol, C. Ersoy, and F. Alagoz, "Mac protocols for wireless sensor networks: a survey," *IEEE Communications Magazine*, vol. 44, no. 4, pp. 115–121, 2006.
- [17] P. Naik and K. M. Sivalingam, "A survey of mac protocols for sensor networks," in *Wireless sensor networks*, pp. 93–107, Springer, 2004.
- [18] P. Huang, L. Xiao, S. Soltani, M. W. Mutka, and N. Xi, "The evolution of mac protocols in wireless sensor networks: A survey," *IEEE communications surveys & tutorials*, vol. 15, no. 1, pp. 101–120, 2013.
- [19] D. Messaoud, D. Djamel, and B. Nadjib, "Survey on latency issues of asynchronous mac protocols in delay-sensitive wireless sensor networks," *IEEE Trans. on Communications Surveys Tutorials*, vol. PP, no. 99, pp. 1–23, 2012.
- [20] P. Suriyachai, U. Roedig, and A. Scott, "A survey of mac protocols for mission-critical applications in wireless sensor networks," *IEEE Communications Surveys & Tutorials*, vol. 14, no. 2, pp. 240–264, 2012.
- [21] S. Kosunalp, "Mac protocols for energy harvesting wireless sensor networks: Survey," *ETRI Journal*, vol. 37, no. 4, pp. 804–812, 2015.
- [22] K. Akkaya and M. Younis, "A survey on routing protocols for wireless sensor networks," *Ad hoc networks*, vol. 3, no. 3, pp. 325–349, 2005.
- [23] S. P. Singh and S. Sharma, "A survey on cluster based routing protocols in wireless sensor networks," *Procedia computer science*, vol. 45, pp. 687–695, 2015.
- [24] D. Goyal and M. R. Tripathy, "Routing protocols in wireless sensor networks: a survey," in *Advanced Computing & Communication Technologies (ACCT), 2012 Second International Conference on*, pp. 474–480, IEEE, 2012.
- [25] N. A. Pantazis, S. A. Nikolidakis, and D. D. Vergados, "Energy-efficient routing protocols in wireless sensor networks: A survey," *IEEE Communications surveys & tutorials*, vol. 15, no. 2, pp. 551–591, 2013.

- [26] S. K. Singh, M. Singh, and D. Singh, "A survey of energy-efficient hierarchical cluster-based routing in wireless sensor networks," *International Journal of Advanced Networking and Application (IJANA)*, vol. 2, no. 02, pp. 570–580, 2010.
- [27] W. K. Seah, Z. A. Eu, and H.-P. Tan, "Wireless sensor networks powered by ambient energy harvesting (wsn-heap)-survey and challenges," in *1st International Conference on Wireless Communication, Vehicular Technology, Information Theory and Aerospace & Electronic Systems Technology, 2009. Wireless VITAE 2009*, pp. 1–5, Ieee, 2009.
- [28] H. Shafieirad, R. S. Adve, and S. ShahbazPanahi, "Large scale energy harvesting sensor networks with applications in smart cities," in *Smart City 360°*, pp. 215–226, Springer, 2016.
- [29] C. Wei and X. Jing, "A comprehensive review on vibration energy harvesting: Modelling and realization," *Renewable and Sustainable Energy Reviews*, vol. 74, pp. 1–18, 2017.
- [30] S. Akbari, "Energy harvesting for wireless sensor networks review," in *2014 Federated Conference on Computer Science and Information Systems (FedCSIS)*, pp. 987–992, IEEE, 2014.
- [31] V. Raghunathan, A. Kansal, J. Hsu, J. Friedman, and M. Srivastava, "Design considerations for solar energy harvesting wireless embedded systems," in *Fourth International Symposium on Information Processing in Sensor Networks, 2005. IPSN 2005*, pp. 457–462, IEEE, 2005.
- [32] J. Taneja, J. Jeong, and D. Culler, "Design, modeling, and capacity planning for micro-solar power sensor networks," in *Proceedings of the 7th international conference on Information processing in sensor networks*, pp. 407–418, IEEE Computer Society, 2008.
- [33] S. Scorcioni, A. Bertacchini, D. Dondi, L. Larcher, P. Pavan, and G. Mainardi, "A vibration-powered wireless system to enhance safety in agricultural machinery," in *37th Annual Conference on IEEE Industrial Electronics Society IECON 2011*, pp. 3510–3515, IEEE, 2011.
- [34] E. S. Leland, E. M. Lai, and P. K. Wright, "A self-powered wireless sensor for indoor environmental monitoring," in *Wireless Networking Symposium, University of Texas at Austin Department of Electrical & Computer Engineering*, 2004.
- [35] N. S. Shenck and J. A. Paradiso, "Energy scavenging with shoe-mounted piezoelectrics," *IEEE micro*, vol. 21, no. 3, pp. 30–42, 2001.
- [36] J. A. Paradiso and M. Feldmeier, "A compact, wireless, self-powered pushbutton controller," in *International Conference on Ubiquitous Computing*, pp. 299–304, Springer, 2001.

- [37] V. Leonov, T. Torfs, P. Fiorini, and C. Van Hoof, "Thermoelectric converters of human warmth for self-powered wireless sensor nodes," *IEEE Sensors Journal*, vol. 7, no. 5, pp. 650–657, 2007.
- [38] Z. Wang, V. Leonov, P. Fiorini, and C. Van Hoof, "Realization of a wearable miniaturized thermoelectric generator for human body applications," *Sensors and Actuators A: Physical*, vol. 156, no. 1, pp. 95–102, 2009.
- [39] X. Lu and S.-H. Yang, "Thermal energy harvesting for wsns," in *2010 IEEE International Conference on Systems Man and Cybernetics (SMC)*, pp. 3045–3052, IEEE, 2010.
- [40] Z. A. Eu, H.-P. Tan, and W. K. G. Seah, "Wireless sensor networks powered by ambient energy harvesting: an empirical characterization," in *2010 IEEE International Conference on Communications (ICC)*, pp. 1–5, IEEE, 2010.
- [41] C. Park and P. H. Chou, "Ambimax: Autonomous energy harvesting platform for multi-supply wireless sensor nodes," in *3rd Annual IEEE Communications Society on Sensor and Ad Hoc Communications and Networks, 2006. SECON'06*, vol. 1, pp. 168–177, IEEE, 2006.
- [42] Y. K. Tan and S. K. Panda, "Optimized wind energy harvesting system using resistance emulator and active rectifier for wireless sensor nodes," *IEEE transactions on power electronics*, vol. 26, no. 1, pp. 38–50, 2011.
- [43] R. Morais, S. G. Matos, M. A. Fernandes, A. L. Valente, S. F. Soares, P. Ferreira, and M. Reis, "Sun, wind and water flow as energy supply for small stationary data acquisition platforms," *Computers and electronics in agriculture*, vol. 64, no. 2, pp. 120–132, 2008.
- [44] H. J. Visser, A. C. Reniers, and J. A. Theeuwes, "Ambient rf energy scavenging: Gsm and wlan power density measurements," in *Microwave Conference, 2008. EuMC 2008. 38th European*, pp. 721–724, IEEE, 2008.
- [45] A. N. Parks, A. P. Sample, Y. Zhao, and J. R. Smith, "A wireless sensing platform utilizing ambient rf energy," in *Biomedical Wireless Technologies, Networks, and Sensing Systems (BioWireless), 2013 IEEE Topical Conference on*, pp. 154–156, IEEE, 2013.
- [46] T. Le, K. Mayaram, and T. Fiez, "Efficient far-field radio frequency energy harvesting for passively powered sensor networks," *IEEE Journal of Solid-State Circuits*, vol. 43, no. 5, pp. 1287–1302, 2008.
- [47] U. Baroudi, S. Mekid, A. Bouhraoua, *et al.*, "Radio frequency energy harvesting characterization: an experimental study," in *Trust, Security and Privacy in Computing and Communications (TrustCom), 2012 IEEE 11th International Conference on*, pp. 1976–1981, IEEE, 2012.

- [48] H. J. Visser and R. J. Vullers, “Rf energy harvesting and transport for wireless sensor network applications: Principles and requirements,” *Proceedings of the IEEE*, vol. 101, no. 6, pp. 1410–1423, 2013.
- [49] R. Zhang and C. K. Ho, “Mimo broadcasting for simultaneous wireless information and power transfer,” *IEEE Transactions on Wireless Communications*, vol. 12, no. 5, pp. 1989–2001, 2013.
- [50] M. Pinuela, P. D. Mitcheson, and S. Lucyszyn, “Ambient rf energy harvesting in urban and semi-urban environments,” *IEEE Transactions on Microwave Theory and Techniques*, vol. 61, no. 7, pp. 2715–2726, 2013.
- [51] A. M. Zungeru, L.-M. Ang, S. Prabaharan, and K. P. Seng, “Radio frequency energy harvesting and management for wireless sensor networks,” *Green Mobile Devices and Networks: Energy Optimization and Scavenging Techniques*, pp. 341–368, 2012.
- [52] “Powercaster transmitter.” <http://www.powercastco.com/products/powercaster-transmitter/>, 2017.
- [53] W. Ye, J. Heidemann, and D. Estrin, “An energy-efficient mac protocol for wireless sensor networks,” in *IEEE INFOCOM 2002. Twenty-First Annual Joint Conference of the IEEE Computer and Communications Societies*, vol. 3, pp. 1567–1576, IEEE, 2002.
- [54] J. Polastre, J. Hill, and D. Culler, “Versatile low power media access for wireless sensor networks,” in *Proceedings of the 2nd international conference on Embedded networked sensor systems*, pp. 95–107, ACM, 2004.
- [55] M. Buettner, G. V. Yee, E. Anderson, and R. Han, “X-mac: a short preamble mac protocol for duty-cycled wireless sensor networks,” in *4th international conference on Embedded networked sensor systems*, pp. 307–320, ACM, 2006.
- [56] D. Moss and P. Levis, “Box-macs: Exploiting physical and link layer boundaries in low-power networking,” *Computer Systems Laboratory Stanford University*, pp. 116–119, 2008.
- [57] A. Dunkels, “The contikimac radio duty cycling protocol,” tech. rep., Swedish Institute of Computer Science, 2011.
- [58] A. El-Hoiydi and J.-D. Decotignie, “Wisemac: An ultra low power mac protocol for multi-hop wireless sensor networks,” in *ALGOSENSORS*, vol. 4, pp. 18–31, Springer, 2004.
- [59] X. Fafoutis, A. Di Mauro, M. D. Vithanage, and N. Dragoni, “Receiver-initiated medium access control protocols for wireless sensor networks,” *Computer Networks*, vol. 76, pp. 55–74, 2015.

- [60] E.-Y. Lin, J. M. Rabaey, and A. Wolisz, "Power-efficient rendez-vous schemes for dense wireless sensor networks," in *IEEE International Conference on Communications*, vol. 7, pp. 3769–3776, IEEE, 2004.
- [61] Y. Sun, O. Gurewitz, and D. B. Johnson, "Ri-mac: a receiver-initiated asynchronous duty cycle mac protocol for dynamic traffic loads in wireless sensor networks," in *Proceedings of the 6th ACM conference on Embedded network sensor systems*, pp. 1–14, ACM, 2008.
- [62] P. Ramezani and M. R. Pakravan, "Overview of mac protocols for energy harvesting wireless sensor networks," in *Personal, Indoor, and Mobile Radio Communications (PIMRC), 2015 IEEE 26th Annual International Symposium on*, pp. 2032–2037, IEEE, 2015.
- [63] X. Fafoutis and N. Dragoni, "Odmac: an on-demand mac protocol for energy harvesting-wireless sensor networks," in *Proceedings of the 8th ACM Symposium on Performance evaluation of wireless ad hoc, sensor, and ubiquitous networks*, pp. 49–56, ACM, 2011.
- [64] K. Nguyen, V.-H. Nguyen, D.-D. Le, Y. Ji, D. A. Duong, and S. Yamada, "Eri-mac: an energy-harvested receiver-initiated mac protocol for wireless sensor networks," *International Journal of Distributed Sensor Networks*, vol. 10, no. 5, p. 514169, 2014.
- [65] F. Iannello, O. Simeone, and U. Spagnolini, "Medium access control protocols for wireless sensor networks with energy harvesting," *IEEE Transactions on Communications*, vol. 60, no. 5, pp. 1381–1389, 2012.
- [66] Z. A. Eu, H.-P. Tan, and W. K. Seah, "Design and performance analysis of mac schemes for wireless sensor networks powered by ambient energy harvesting," *Ad Hoc Networks*, vol. 9, no. 3, pp. 300–323, 2011.
- [67] P. Nintanavongsa, "A survey on rf energy harvesting: circuits and protocols," *Energy Procedia*, vol. 56, pp. 414–422, 2014.
- [68] K. W. Choi, L. Ginting, P. A. Rosyady, A. A. Aziz, and D. I. Kim, "Wireless-powered sensor networks: How to realize," *IEEE Transactions on Wireless Communications*, vol. 16, no. 1, pp. 221–234, 2017.
- [69] X. Lu, P. Wang, D. Niyato, and Z. Han, "Resource allocation in wireless networks with rf energy harvesting and transfer," *IEEE Network*, vol. 29, no. 6, pp. 68–75, 2015.
- [70] M. Y. Naderi, P. Nintanavongsa, and K. R. Chowdhury, "Rf-mac: A medium access control protocol for re-chargeable sensor networks powered by wireless energy harvesting," *IEEE Transactions on Wireless Communications*, vol. 13, no. 7, pp. 3926–3937, 2014.



- [71] P. Tamilarasi and B. Lavenya, "Energy and throughput enhancement in wireless powered communication networks using rf-mac and csma," in *Innovations in Information, Embedded and Communication Systems (ICIIECS), 2015 International Conference on*, pp. 1–4, IEEE, 2015.
- [72] J. Kim and J.-W. Lee, "Energy adaptive mac protocol for wireless sensor networks with rf energy transfer," in *2011 Third International Conference on Ubiquitous and Future Networks (ICUFN)*, pp. 89–94, IEEE, 2011.
- [73] R. Shigeta, T. Sasaki, D. M. Quan, Y. Kawahara, R. J. Vyas, M. M. Tentzeris, and T. Asami, "Ambient rf energy harvesting sensor device with capacitor-leakage-aware duty cycle control," *IEEE Sensors Journal*, vol. 13, no. 8, pp. 2973–2983, 2013.
- [74] W. K. Seah and J. P. Olds, "Data delivery scheme for wireless sensor network powered by rf energy harvesting," in *2013 IEEE Wireless Communications and Networking Conference (WCNC)*, pp. 1498–1503, IEEE, 2013.
- [75] H. Chen, L. Cui, and V. O. Li, "A joint design of opportunistic forwarding and energy-efficient mac protocol in wireless sensor networks," in *Global Telecommunications Conference*, pp. 1–6, IEEE, 2009.
- [76] X. Fafoutis, A. Di Mauro, C. Orfanidis, and N. Dragoni, "Energy-efficient medium access control for energy harvesting communications," *IEEE transactions on consumer electronics*, vol. 61, no. 4, pp. 402–410, 2015.
- [77] E. G. Barrabes, "Opportunistic routing for indoor energy harvesting wireless sensor networks," Master's thesis, Delft University of Technology, the Netherlands, 2016.
- [78] Z. A. Eu, H.-P. Tan, and W. K. Seah, "Opportunistic routing in wireless sensor networks powered by ambient energy harvesting," *Computer Networks*, vol. 54, no. 17, pp. 2943–2966, 2010.
- [79] S. Liu, K.-W. Fan, and P. Sinha, "Cmac: An energy-efficient mac layer protocol using convergent packet forwarding for wireless sensor networks," *ACM Transactions on Sensor Networks (TOSN)*, vol. 5, no. 4, p. 29, 2009.
- [80] O. Landsiedel, E. Ghadimi, S. Duquennoy, and M. Johansson, "Low power, low delay: opportunistic routing meets duty cycling," in *11th International Conference on Information Processing in Sensor Networks (IPSN)*, pp. 185–196, IEEE, 2012.
- [81] M. Tacca, P. Monti, and A. Fumagalli, "Cooperative and reliable arq protocols for energy harvesting wireless sensor nodes," *IEEE Transactions on Wireless Communications*, vol. 6, no. 7, pp. 2519–2529, 2007.

- [82] M. Yoshida, T. Kitani, M. Bandai, T. Watanabe, P. H. Chou, and W. K. Seah, "Probabilistic data collection protocols for energy harvesting wireless sensor networks," *International Journal of Ad Hoc and Ubiquitous Computing*, vol. 11, no. 2-3, pp. 82–96, 2012.
- [83] K. Tutuncuoglu and A. Yener, "Short-term throughput maximization for battery limited energy harvesting nodes," in *2011 IEEE International Conference on Communications (ICC)*, pp. 1–5, IEEE, 2011.
- [84] S. Rashwand, J. Mistic, V. Mistic, S. Biswas, and M. M. Haque, "A novel asynchronous, energy efficient, low transmission delay mac protocol for wireless sensor networks," in *Distributed Computing Systems Workshops, 2009. ICDCS Workshops' 09. 29th IEEE International Conference on*, pp. 186–193, IEEE, 2009.
- [85] X. Wang, X. Zhang, G. Chen, and Q. Zhang, "Opportunistic cooperation in low duty cycle wireless sensor networks," in *Communications (ICC), 2010 IEEE International Conference on*, pp. 1–5, IEEE, 2010.
- [86] A. Arora, P. Dutta, S. Bapat, V. Kulathumani, H. Zhang, V. Naik, V. Mittal, H. Cao, M. Demirbas, M. Gouda, *et al.*, "A line in the sand: a wireless sensor network for target detection, classification, and tracking," *Computer Networks*, vol. 46, no. 5, pp. 605–634, 2004.
- [87] M. Bahrepour, N. Meratnia, M. Poel, Z. Taghikhaki, and P. J. Havinga, "Distributed event detection in wireless sensor networks for disaster management," in *2nd International Conference on Intelligent Networking and Collaborative Systems (INCOS), 2010*, pp. 507–512, IEEE, 2010.
- [88] D. Moss, J. Hui, and K. Klues, "Low power listening," *TinyOS Core Working Group, TEP*, vol. 105, 2007.
- [89] W. J. Stewart, *Probability, Markov chains, queues, and simulation: the mathematical basis of performance modeling*. Princeton University Press, 2009.
- [90] U. Wilensky, "Netlogo." <http://ccl.northwestern.edu/netlogo/>. Center for Connected Learning and Computer-Based Modeling, Northwestern University. Evanston, IL, 1999. Accessed: Oct 14, 2014.
- [91] "Micaz data sheet." [www.memsic.com/userfiles/files/Datasheets/WSN/micaz\\_datasheet-t.pdf](http://www.memsic.com/userfiles/files/Datasheets/WSN/micaz_datasheet-t.pdf), 2017.
- [92] R. Jurdak, A. G. Ruzzelli, and G. M. O'Hare, "Radio sleep mode optimization in wireless sensor networks," *IEEE Transactions on Mobile Computing*, vol. 9, no. 7, pp. 955–968, 2010.
- [93] M. Krämer and A. Gerald, "Energy measurements for micaz node," *University of Kaiserslautern, Kaiserslautern, Germany, Technical Report KrGe06*, 2006.

- [94] D. Pediaditakis, Y. Tselishchev, and A. Boulis, "Performance and scalability evaluation of the castalia wireless sensor network simulator," in *Proceedings of the 3rd International ICST Conference on Simulation Tools and Techniques*, p. 53, ICST (Institute for Computer Sciences, Social-Informatics and Telecommunications Engineering), 2010.
- [95] M. M. I. Rajib and A. Nasipuri, "Delay performance of intermittently connected wireless sensor networks with cooperative relays," in *International Conference on Communication Workshop (ICCW)*, pp. 1994–1999, IEEE, 2015.
- [96] K. Kaushik, D. Mishra, S. De, S. Basagni, W. Heinzelman, K. Chowdhury, and S. Jana, "Experimental demonstration of multi-hop rf energy transfer," in *IEEE 24th International Symposium on Personal Indoor and Mobile Radio Communications (PIMRC)*, pp. 538–542, IEEE, 2013.
- [97] S. De and R. Singhal, "Toward uninterrupted operation of wireless sensor networks," *Computer*, vol. 45, no. 9, pp. 24–30, 2012.
- [98] "Powercast development kit." <http://www.powercastco.com/products/development-kits/#P2110-EVAL-01>, 2017.
- [99] D. P. Bertsekas and J. N. Tsitsiklis, *Introduction to probability*, vol. 1. Athena Scientific Belmont, MA, 2008.